

Chapter 11

Aerodynamics

Antony Jameson

Stanford University, Stanford, USA

1 Focus and Historical Background	1
2 Mathematical Models of Fluid Flow	6
3 Potential Flow Methods	10
4 Shock-capturing Algorithms for the Euler and Navier–Stokes Equations	25
5 Discretization Scheme for Flows in Complex Multidimensional Domains	36
6 Time-stepping Schemes	42
7 Aerodynamic Shape Optimization	57
Acknowledgment	76
References	76

1 FOCUS AND HISTORICAL BACKGROUND

1.1 Classical aerodynamics

This article surveys some of the principal developments of computational aerodynamics, with a focus on aeronautical applications. It is written with the perspective that computational mathematics is a natural extension of classical methods of applied mathematics, which has enabled the treatment of more complex, in particular nonlinear, mathematical models, and also the calculation of solutions in very complex geometric domains, not amenable to classical techniques such as the separation of variables.

Encyclopedia of Computational Mechanics, Edited by Erwin Stein, René de Borst and Thomas J.R. Hughes. Volume 3: *Computational Fluid Dynamics*. © 2004 John Wiley & Sons, Ltd. ISBN: 0-470-84699-2.

This is particularly true for aerodynamics. Efficient flight can be achieved only by establishing highly coherent flows. Consequently, there are many important applications where it is not necessary to solve the full Navier–Stokes equations in order to gain an insight into the nature of the flow, and useful predictions can be made with simplified mathematical models. It was already recognized by Prandtl (1904), and Schlichting and Gersten (1999), essentially contemporaneous with the first successful flights of the Wright brothers, that in flows at the large Reynolds numbers typical of powered flight, viscous effects are important chiefly in thin shear layers adjacent to the surface. While these boundary layers play a critical role in determining whether the flow will separate and how much circulation will be generated around a lifting surface, the equations of inviscid flow are a good approximation in the bulk of the flow field external to the boundary layer. In the absence of separation, a first estimate of the effect of the boundary layer is provided by regarding it as increasing the effective thickness of the body. This procedure can be justified by asymptotic analysis (Van Dyke, 1964; Ashley and Landahl, 1965).

The classical treatment of the external inviscid flow is based on Kelvin's theorem that in the absence of discontinuities the circulation around a material loop remains constant. Consequently, an initially irrotational flow remains irrotational. This allows us to simplify the equations further by representing the velocity as the gradient of a potential. If the flow is also regarded as incompressible, the governing equation reduces to Laplace's equation. These simplifications provided the basis for the classical airfoil theory of Glauert (1926) and Prandtl's wing theory (Ashley and Landahl, 1965; Prandtl and Tietjens, 1934). Supersonic flow over slender bodies at Mach numbers greater than two is also well represented by the linearized equations. Techniques for the solution of linearized flow were perfected in

the period 1935–1950, particularly by Hayes, who derived the supersonic area rule (Hayes, 1947).

Classical aerodynamic theory provided engineers with a good insight into the nature of the flow phenomena, and a fairly good estimate of the force on simple configurations such as an isolated wing, but could not predict the details of the flow over the complex configuration of a complete aircraft. Consequently, the primary tool for the development of aerodynamic configurations was the wind tunnel. Shapes were tested and modifications selected in the light of pressure and force measurements together with flow visualization techniques. In much the same way that Michelangelo, della Porta, and Fontana could design the dome of St. Peters through a good physical understanding of stress paths, so could experienced aerodynamicists arrive at efficient shapes through testing guided by good physical insight. Notable examples of the power of this method include the achievement of the Wright brothers in leaving the ground (after first building a wind tunnel), and more recently Whitcomb's discovery of the area rule for transonic flow, followed by his development of aft-loaded supercritical airfoils and winglets (Whitcomb, 1956; Whitcomb, 1974; Whitcomb, 1976). The process was expensive. More than 20 000 hours of wind-tunnel testing were expended in the development of some modern designs, such as the Boeing 747.

1.2 The emergence of computational aerodynamics and its application to transonic flow

Prior to 1960, computational methods were hardly used in aerodynamic analysis, although they were already widely used for structural analysis. The NACA 6 series of airfoils had been developed during the forties, using hand computation to implement the Theodorsen method for conformal mapping (Theodorsen, 1931). The first major success in computational aerodynamics was the introduction of boundary integral methods by Hess and Smith (1962) to calculate potential flow over an arbitrary configuration. Generally known in the aeronautical community as panel methods, these continue to be used to the present day to make initial predictions of low speed aerodynamic characteristics of preliminary designs. It was the compelling need, however, both to predict transonic flow and to gain a better understanding of its properties and character that was a driving force for the development of computational aerodynamics through the period 1970 to 1990.

In the case of military aircraft capable of supersonic flight, the high drag associated with high g maneuvers

forces them to be performed in the transonic regime. In the case of commercial aircraft, the importance of transonic flow stems from the Breguet range equation. This provides a good first estimate of range as

$$R = \frac{V}{sfc} \frac{L}{D} \log \frac{W_0 + W_f}{W_0} \quad (1)$$

Here V is the speed, L/D is the lift to drag ratio, sfc is the specific fuel consumption of the engines, W_0 is the landing weight, and W_f is the weight of the fuel burnt. The Breguet equation clearly exposes the multidisciplinary nature of the design problem. A lightweight structure is needed to minimize W_0 . The specific fuel consumption is mainly the province of the engine manufacturers, and in fact, the largest advances during the last 30 years have been in engine efficiency. The aerodynamic designer should try to maximize VL/D . This means that the cruising speed should be increased until the onset of drag rise due to the formation of shock waves. Consequently, the best cruising speed is the transonic regime. The typical pattern of transonic flow over a wing section is illustrated in Figure 1.

Transonic flow had proved essentially intractable to analytic methods. Garabedian and Korn had demonstrated the feasibility of designing airfoils for shock-free flow in the transonic regime numerically by the method of complex characteristics (Bauer, Garabedian and Korn, 1972). Their method was formulated in the hodograph plane, and it required great skill to obtain solutions corresponding to physically realizable shapes. It was also known from Morawetz's theorem (Morawetz, 1956) that shock-free transonic solutions are isolated points.

A major breakthrough was accomplished by Murman and Cole (1971) with their development of type-dependent differencing in 1970. They obtained stable solutions by simply switching from central differencing in the subsonic zone to upwind differencing in the supersonic zone and using

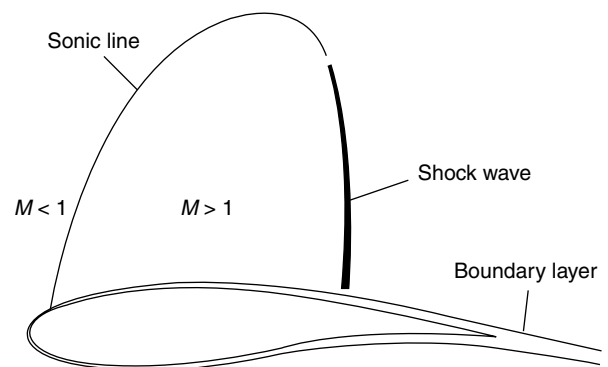


Figure 1. Transonic flow past an airfoil.

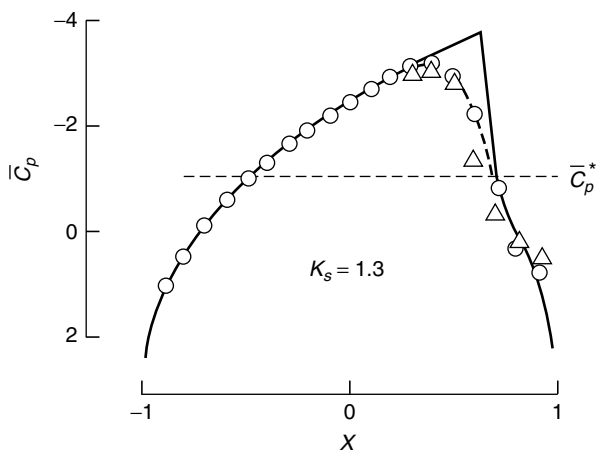


Figure 2. Scaled pressure coefficient on surface of a thin, circular-arc airfoil in transonic flow, compared with experimental data; solid line represents computational result.

a line-implicit relaxation scheme. Their discovery provided major impetus for the further development of computational fluid dynamics (CFD) by demonstrating that solutions for steady transonic flows could be computed economically. Figure 2 taken from their landmark paper illustrates the scaled pressure distribution on the surface of a symmetric airfoil. Efforts were soon underway to extend their ideas to more general transonic flows.

Numerical methods to solve transonic potential flow over complex configurations were essentially perfected during the period 1970 to 1982. The AIAA First Computational Fluid Dynamics Conference, held in Palm Springs in July 1973, signified the emergence of CFD as an accepted tool for airplane design, and seems to mark the first use of the name CFD. The rotated difference scheme for transonic potential flow, first introduced by the author at this conference, proved to be a very robust method, and it provided the basis for the computer program flo22, developed with David Caughey during 1974 to 1975 to predict transonic flow past swept wings. At the time we were using the CDC 6600, which had been designed by Seymour Cray and was the world's fastest computer at its introduction, but had only 131 000 words of memory. This forced the calculation to be performed one plane at a time, with multiple transfers from the disk. Flo22 was immediately put into use at McDonnell Douglas. A simplified in-core version of flo22 is still in use at Boeing Long Beach today. Figure 3, shows the result of a recent calculation, using flo22, of transonic flow over the wing of a proposed aircraft to fly in the Martian atmosphere. The result was obtained with 100 iterations on a $192 \times 32 \times 32$ mesh in 7 seconds, using a typical modern workstation. When flo22 was first introduced at Long Beach, the calculations cost \$3000 each. Nevertheless, they found it worthwhile to use it

extensively for the aerodynamic design of the C17 military cargo aircraft.

In order to treat complete configurations, it was necessary to develop discretization formulas for arbitrary grids. An approach that proved successful (Jameson and Caughey, 1977), is to derive the discretization formulas from the Bateman variational principle that the integral of the pressure over the domain,

$$I = \int_D p \, d\xi$$

is stationary (Jameson, 1978). The resulting scheme is essentially a finite element scheme using trilinear isoparametric elements. It can be stabilized in the supersonic zone by the introduction of artificial viscosity to produce an upwind bias. The 'hour-glass' instability that results from the use of one point integration scheme is suppressed by the introduction of higher-order coupling terms based on mixed derivatives. The flow solvers (flo27-30) based on this approach were subsequently incorporated in Boeing's A488 software, which was used in the aerodynamic design of Boeing commercial aircraft throughout the eighties (Rubbert, 1994).

In the same period, Perrier was focusing the research efforts at Dassault on the development of finite element methods using triangular and tetrahedral meshes, because he believed that if CFD software was to be really useful for aircraft design, it must be able to treat complete configurations. Although finite element methods were more computationally expensive, and mesh generation continued to present difficulties, finite element methods offered a route toward the achievement of this goal. The Dassault/INRIA group was ultimately successful, and they performed transonic potential flow calculations for complete aircraft such as the Falcon 50 in the early eighties (Bristeau *et al.*, 1985).

1.3 The development of methods for the Euler and Navier–Stokes equations

By the eighties, advances in computer hardware had made it feasible to solve the full Euler equations using software that could be cost-effective in industrial use. The idea of directly discretizing the conservation laws to produce a finite volume scheme had been introduced by MacCormack and Paullay (1972). Most of the early flow solvers tended to exhibit strong pre- or post-shock oscillations. Also, in a workshop held in Stockholm in 1979, (Rizzi and Viviani, 1979) it was apparent that none of the existing schemes converged to a steady state. These difficulties were resolved during the following decade.

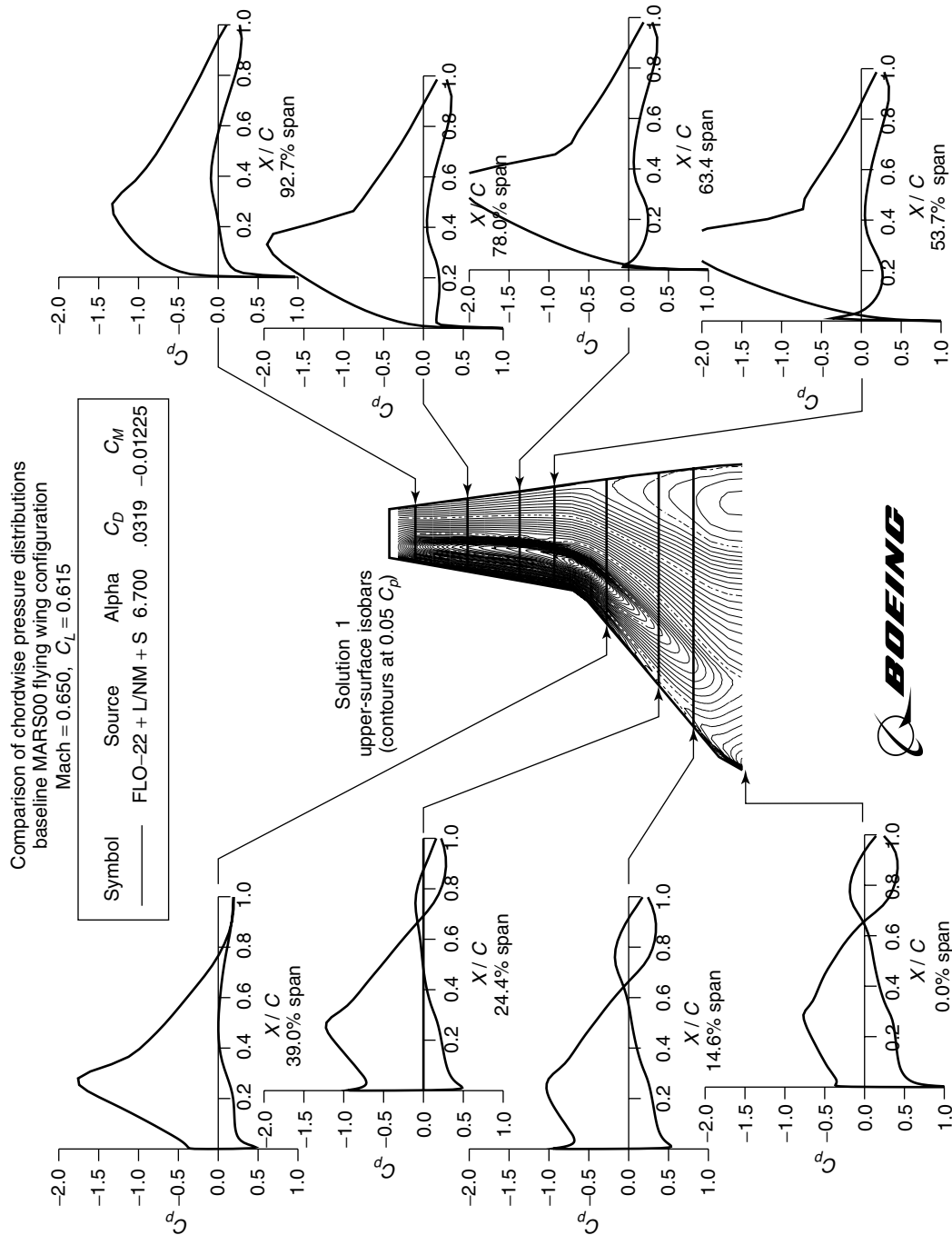


Figure 3. Pressure distribution over the wing of a Mars Lander using flo22 (supplied by John Vassberg).

The Jameson–Schmidt–Turkel (JST) scheme (Jameson, Schmidt and Turkel, 1981a), which used Runge–Kutta time stepping and a blend of second- and fourth-differences (both to control oscillations and to provide background dissipation), consistently demonstrated convergence to a steady state, with the consequence that it has remained one of the most widely used methods to the present day.

A fairly complete understanding of shock-capturing algorithms was achieved, stemming from the ideas of Godunov, Van Leer, Harten, and Roe. The issue of oscillation control and positivity had already been addressed by Godunov (1959) in his pioneering work in the 1950s (translated into English in 1959). He had introduced the concept of representing the flow as piecewise constant in each computational cell, and solving a Riemann problem at each interface, thus obtaining a first-order accurate solution that avoids nonphysical features such as expansion shocks. When this work was eventually recognized in the West, it became very influential. It was also widely recognized that numerical schemes might benefit from distinguishing the various wave speeds, and this motivated the development of characteristics-based schemes.

The earliest higher-order characteristics-based methods used flux vector splitting (Steger and Warming, 1981), but suffered from oscillations near discontinuities similar to those of central-difference schemes in the absence of numerical dissipation. The monotone upwind scheme for conservation laws (MUSCL) of Van Leer (1974) extended the monotonicity-preserving behavior of Godunov’s scheme to higher order through the use of limiters. The use of limiters dates back to the flux-corrected transport (FCT) scheme of Boris and Book (1973). A general framework for oscillation control in the solution of nonlinear problems was provided by Harten’s concept of total variation diminishing (TVD) schemes. It finally proved possible to give a rigorous justification of the JST scheme (Jameson, 1995a; Jameson, 1995b).

Roe’s introduction of the concept of locally linearizing the equations through a mean value Jacobian (Roe, 1981) had a major impact. It provided valuable insight into the nature of the wave motions and also enabled the efficient implementation of Godunov-type schemes using approximate Riemann solutions. Roe’s flux-difference splitting scheme has the additional benefit that it yields a single-point numerical shock structure for stationary normal shocks. Roe’s and other approximate Riemann solutions, such as that due to Osher, have been incorporated in a variety of schemes of Godunov type, including the essentially nonoscillatory (ENO) schemes of Harten *et al.* (1987).

Solution methods for the Reynolds-averaged Navier–Stokes (RANS) equations had been pioneered in the seventies by MacCormack and others, but at that time they were extremely expensive. By the nineties, computer technology had progressed to the point where RANS simulations could be performed with manageable costs, and they began to be fairly widely used by the aircraft industry. The need for robust and reliable methods to predict hypersonic flows, which contain both very strong shock wave and near vacuum regions, gave a further impetus to the development of advanced shock-capturing algorithms for compressible viscous flow.

1.4 Overview of the article

The development of software for aerodynamic simulation can be broken down into five main steps.

1. The choice of a mathematical model that represents the physical phenomena that are important for the application;
2. mathematical analysis of the model to ensure existence and uniqueness of the solutions;
3. formulation of a stable and convergent discretization scheme;
4. implementation in software;
5. validation.

Thorough validation is difficult and time consuming. It should include verification procedures for program correctness and consistency checks. For example, does the numerical solution of a symmetric profile at zero angle of attack preserve the symmetry, with no lift? It should also include mesh refinement studies to verify convergence and, ideally, comparisons with the results of other computer programs that purport to solve the same equations. Finally, if it is sufficiently well established that the software provides an accurate solution of the chosen mathematical model, comparisons with experimental data should show whether the model adequately represents the true physics or establish its range of applicability.

This article is primarily focused on the third step, discretization. The complexity of predicting highly nonlinear transonic and hypersonic flows has forced the emergence of an entirely new class of numerical algorithms and a supporting body of theory, which is reviewed in this article. Section 2 presents a brief survey of the mathematical models of fluid flow that are relevant to different flight regimes. Section 3 surveys potential flow methods, which continue to be useful for preliminary design because of their low computational costs and rapid turn around. Section 4 focuses on the formulation of shock-capturing methods

for the Euler and RANS equations. Section 5 discusses alternative ways to discretize the equations in complex geometric domains using either structured or unstructured meshes. Section 6 discusses time-stepping schemes, including convergence acceleration techniques for steady flows and the formulation of accurate and efficient time-stepping techniques for unsteady flows. The article concludes with a discussion of methods to solve inverse and optimum shape-design problems.

2 MATHEMATICAL MODELS OF FLUID FLOW

The Navier–Stokes equations state the laws of conservation of mass, momentum, and energy for the flow of a gas in thermodynamic equilibrium. In the Cartesian tensor notation, let x_i be the coordinates, p , ρ , T , and E the pressure, density, temperature, and total energy, and u_i the velocity components. Each conservation equation has the form

$$\frac{\partial w}{\partial t} + \frac{\partial f_j}{\partial x_j} = 0 \quad (2)$$

For the mass equation

$$w = \rho, \quad f_j = \rho u_j \quad (3)$$

For the i momentum equation

$$w_i = \rho u_i, \quad f_{ij} = \rho u_i u_j + p \delta_{ij} - \sigma_{ij} \quad (4)$$

where σ_{ij} is the viscous stress tensor, which for a Newtonian fluid is proportional to the rate of strain tensor and the bulk dilatation. If μ and λ are the coefficients of viscosity and bulk viscosity, then

$$\sigma_{ij} = \mu \left(\frac{\partial u_i}{\partial x_j} + \frac{\partial u_j}{\partial x_i} \right) + \lambda \delta_{ij} \left(\frac{\partial u_k}{\partial x_k} \right) \quad (5)$$

Typically $\lambda = -2\mu/3$. For the energy equation

$$w = \rho E, \quad f_j = \rho H u_j - \sigma_{jk} u_k - \kappa \frac{\partial T}{\partial x_j} \quad (6)$$

where κ is the coefficient of heat conduction and H is the total enthalpy,

$$H = E + \frac{p}{\rho}$$

In the case of a perfect gas, the pressure is related to the density and energy by the equation of state

$$p = (\gamma - 1)\rho \left(E - \frac{1}{2}q^2 \right) \quad (7)$$

where

$$q^2 = u_i u_i$$

and γ is the ratio of specific heats. The coefficient of thermal conductivity and the temperature satisfy the relations

$$k = \frac{c_p \mu}{Pr}, \quad T = \frac{p}{R\rho} \quad (8)$$

where c_p is the specific heat at constant pressure, R is the gas constant, and Pr is the Prandtl number. Also the speed of sound c is given by the ratio

$$c^2 = \frac{\gamma p}{\rho} \quad (9)$$

and a key dimensionless parameter governing the effects of compressibility is the Mach number

$$M = \frac{q}{c}$$

where q is the magnitude of the velocity.

If the flow is inviscid, the boundary condition that must be satisfied at a solid wall is

$$\mathbf{u} \cdot \mathbf{n} = u_i n_i = 0 \quad (10)$$

where \mathbf{n} denotes the normal to the surface. Viscous flows must satisfy the ‘no-slip’ condition

$$\mathbf{u} = 0 \quad (11)$$

Viscous solutions also require a boundary condition for the energy equation. The usual practice in pure aerodynamic simulations is either to specify the isothermal condition

$$T = T_0 \quad (12)$$

or to specify the adiabatic condition

$$\frac{\partial T}{\partial n} = 0 \quad (13)$$

corresponding to zero heat transfer. The calculation of heat transfer requires an appropriate coupling to a model of the structure.

For an external flow, the flow variables should approach free-stream values

$$p = p_\infty, \quad \rho = \rho_\infty, \quad T = T_\infty, \quad \mathbf{u} = \mathbf{u}_\infty$$

for upstream at the inflow boundary. If any entropy is generated, the density for downstream at the outflow boundary cannot recover to ρ_∞ if the pressure recovers to p_∞ . In fact, if trailing vortices persist downstream, the pressure does not recover to p_∞ . In general, it is necessary to examine the incoming and outgoing waves at the outer boundaries of the flow domain. Boundary values should then only be imposed for quantities transported by the incoming waves. In a subsonic flow, there are four incoming waves at the inflow boundary, and one escaping acoustic wave. Correspondingly, four quantities should be specified. At the outflow boundary, there are four outgoing waves, so one quantity should be specified. One way to do this is to introduce Riemann invariants corresponding to a one-dimensional flow normal to the boundary, as will be discussed in Section 5.4. In a supersonic flow, all quantities should be fixed at the inflow boundary, while they should all be extrapolated at the outflow boundary. The proper specification of inflow and outflow boundary conditions is particularly important in the calculation of internal flows. Otherwise spurious wave reflections may severely corrupt the solution.

In smooth regions of the flow, the inviscid equations can be written in quasilinear form as

$$\frac{\partial w}{\partial t} + A_i \frac{\partial w}{\partial x_i} = 0 \quad (14)$$

where A_i are the Jacobians $\partial f_i / \partial w$. By transforming to the symmetrizing variables, which may be written in differential form as

$$d\tilde{w} = \left(\frac{dp}{\rho c}, du_1, du_2, du_3, dp - c^2 d\rho \right)^T \quad (15)$$

the Jacobians assume the symmetric form

$$\tilde{A}_i = \begin{bmatrix} u_i & \delta_{i1}c & \delta_{i2}c & \delta_{i3}c & 0 \\ \delta_{i1}c & u_i & 0 & 0 & 0 \\ \delta_{i2}c & 0 & u_i & 0 & 0 \\ \delta_{i3}c & 0 & 0 & u_i & 0 \\ 0 & 0 & 0 & 0 & u_i \end{bmatrix} \quad (16)$$

where δ_{ij} are the Kronecker deltas. Equation (14) becomes

$$\frac{\partial \tilde{w}}{\partial t} + \tilde{A}_i \frac{\partial \tilde{w}}{\partial x_i} = 0 \quad (17)$$

The Jacobians for the conservative variables may now be expressed as

$$A_i = T \tilde{A}_i T^{-1} \quad (18)$$

where

$$T^{-1} = \frac{\partial \tilde{w}}{\partial w} = \begin{bmatrix} (\gamma-1) \frac{q^2}{2\rho c} & -(\gamma-1) \frac{u_1}{\rho c} & -(\gamma-1) \frac{u_2}{\rho c} & -(\gamma-1) \frac{u_3}{\rho c} & \frac{\gamma-1}{\rho c} \\ -\frac{u_1}{\rho} & \frac{1}{\rho} & 0 & 0 & 0 \\ -\frac{u_2}{\rho} & 0 & \frac{1}{\rho} & 0 & 0 \\ -\frac{u_3}{\rho} & 0 & 0 & \frac{1}{\rho} & 0 \\ (\gamma-1) \frac{q^2}{2} - c^2 & -(\gamma-1)u_1 & -(\gamma-1)u_2 & -(\gamma-1)u_3 & \gamma-1 \end{bmatrix}$$

and

$$T = \frac{\partial w}{\partial \tilde{w}} = \begin{bmatrix} \frac{\rho}{c} & 0 & 0 & 0 & -\frac{1}{c^2} \\ \frac{\rho u_1}{c} & \rho & 0 & 0 & -\frac{u_1}{c^2} \\ \frac{\rho u_2}{c} & 0 & \rho & 0 & -\frac{u_2}{c^2} \\ \frac{\rho u_3}{c} & 0 & 0 & \rho & -\frac{u_3}{c^2} \\ \frac{\rho H}{c} & \rho u_1 & \rho u_2 & \rho u_3 & -\frac{q^2}{2c^2} \end{bmatrix} \quad (19)$$

The decomposition (17) clearly exposes the wave structure in solutions of the gas-dynamic equations. The wave speeds appear as the eigenvalues of the linear combination

$$\tilde{A} = n_i \tilde{A}_i \quad (20)$$

where \mathbf{n} is a unit direction vector. They are

$$[q_n + c, q_n - c, q_n, q_n, q_n]^T \quad (21)$$

where $q_n = \mathbf{q} \cdot \mathbf{n}$. Corresponding to the fact that \tilde{A} is symmetric, one can find a set of orthogonal eigenvectors, which may be normalized to unit length. Then one can express

$$\tilde{A} = \tilde{M} \Lambda \tilde{M}^{-1} \quad (22)$$

where Λ is diagonal, with the eigenvalues as its elements. The modal matrix \tilde{M} containing the eigenvectors as its

columns is

$$\tilde{M} = \begin{bmatrix} \frac{1}{\sqrt{2}} & -\frac{1}{\sqrt{2}} & 0 & 0 & 0 \\ \frac{n_1}{\sqrt{2}} & \frac{n_1}{\sqrt{2}} & 0 & -n_3 & n_2 \\ \frac{n_2}{\sqrt{2}} & \frac{n_2}{\sqrt{2}} & n_3 & 0 & -n_1 \\ \frac{n_3}{\sqrt{2}} & \frac{n_3}{\sqrt{2}} & -n_2 & n_1 & 0 \\ 0 & 0 & n_1 & n_2 & n_3 \end{bmatrix} \quad (23)$$

and $\tilde{M}^{-1} = \tilde{M}^T$. The Jacobian matrix $A = n_i A_i$ now takes the form

$$A = M \Lambda M^{-1} \quad (24)$$

where

$$M = T \tilde{M}, \quad M^{-1} = \tilde{M}^T T^{-1} \quad (25)$$

In the design of difference schemes, it proves useful to introduce the absolute Jacobian matrix $|A|$, in which the eigenvalues are replaced by their absolute values, as will be discussed in Section 4.4.

Corresponding to the thermodynamic relation

$$\frac{dp}{\rho} = dh - T dS$$

where S is the entropy $\log(p/\rho^\gamma)$, the last variable of $d\tilde{w}$ corresponds to $p dS$, since $c^2 = (dp/d\rho)$. It follows that in the absence of shock waves S is constant along streamlines. If the flow is isentropic, then $(dp/d\rho) \propto \rho^{\gamma-1}$, and the first variable can be integrated to give $2c/(\gamma-1)$. Then we may take the transformed variables as

$$\tilde{w} = \left(\frac{2c}{\gamma-1}, u_1, u_2, u_3, S \right)^T \quad (26)$$

In the case of a one-dimensional flow, the equations for the Riemann invariants are recovered by adding and subtracting the equations for $2c/(\gamma-1)$ and u_1 .

In order to calculate solutions for flows in complex geometric domains, it is often useful to introduce body-fitted coordinates through global, or, as in the case of isoparametric elements, local transformations. With the body now coinciding with a coordinate surface, it is much easier to enforce the boundary conditions accurately. Suppose that the mapping to computational coordinates (ξ_1, ξ_2, ξ_3) is defined by the transformation matrices

$$K_{ij} = \frac{\partial x_i}{\partial \xi_j}, \quad K_{ij}^{-1} = \frac{\partial \xi_i}{\partial x_j}, \quad J = \det(K) \quad (27)$$

The Navier–Stokes equations (2–6) become

$$\frac{\partial}{\partial t}(Jw) + \frac{\partial}{\partial \xi_i} F_i(w) = 0 \quad (28)$$

Here the transformed fluxes are

$$F_i = S_{ij} f_j \quad (29)$$

where

$$S = JK^{-1} \quad (30)$$

The elements of S are the cofactors of K , and in a finite volume discretization, they are just the face areas of the computational cells projected in the x_1 , x_2 , and x_3 directions. Using the permutation tensor ϵ_{ijk} we can express the elements of S as

$$S_{ij} = \frac{1}{2} \epsilon_{j pq} \epsilon_{irs} \frac{\partial x_p}{\partial \xi_r} \frac{\partial x_q}{\partial \xi_s} \quad (31)$$

Then

$$\begin{aligned} \frac{\partial}{\partial \xi_i} S_{ij} &= \frac{1}{2} \epsilon_{j pq} \epsilon_{irs} \left(\frac{\partial^2 x_p}{\partial \xi_r \partial \xi_i} \frac{\partial x_q}{\partial \xi_s} + \frac{\partial x_p}{\partial \xi_r} \frac{\partial^2 x_q}{\partial \xi_s \partial \xi_i} \right) \\ &= 0 \end{aligned} \quad (32)$$

Defining scaled contravariant velocity components as

$$U_i = S_{ij} u_j \quad (33)$$

the flux formulas may be expanded as

$$F_i = \begin{Bmatrix} \rho U_i \\ \rho U_i u_1 + S_{i1} p \\ \rho U_i u_2 + S_{i2} p \\ \rho U_i u_3 + S_{i3} p \\ \rho U_i H \end{Bmatrix} \quad (34)$$

If we choose a coordinate system so that the boundary is at $\xi_l = 0$, the wall boundary condition for inviscid flow is now

$$U_i = 0 \quad (35)$$

An indication of the relative magnitude of the inertial and viscous terms is given by the Reynolds number

$$Re = \frac{\rho U L}{\mu} \quad (36)$$

where U is a characteristic velocity and L a representative length. The viscosity of air is very small, and typical

Reynolds numbers for the flow past a component of an aircraft such as a wing are of the order of 10^7 or more, depending on the size and speed of the aircraft. In this situation, the viscous effects are essentially confined to thin boundary layers covering the surface. Boundary layers may nevertheless have a global impact on the flow by causing separation. Unfortunately, unless they are controlled by active means such as suction through a porous surface, boundary layers are unstable and generally become turbulent.

Using dimensional analysis, Kolmogorov's theory of turbulence (Kolmogorov, 1941) estimates the length scales of the smallest persisting eddies to be of order $(1/Re^{3/4})$ in comparison with the macroscopic length scale of the flow. Accordingly the computational requirements for the full simulation of all scales of turbulence can be estimated as growing proportionally to $Re^{9/4}$, and are clearly beyond the reach of current computers. Turbulent flows may be simulated by the RANS equations, where statistical averages are taken of rapidly fluctuating components. Denoting fluctuating parts by primes and averaging by an overbar, this leads to the appearance of Reynolds stress terms of the form $\overline{\rho u'_i u'_j}$, which cannot be determined from the mean values of the velocity and density. Estimates of these additional terms must be provided by a turbulence model. The simplest turbulence models augment the molecular viscosity by an eddy viscosity that crudely represents the effects of turbulent mixing, and is estimated with some characteristic length scale such as the boundary layer thickness. A rather more elaborate class of models introduces two additional equations for the turbulent kinetic energy and the rate of dissipation. Existing turbulence models are adequate for particular classes of flow for which empirical correlations are available, but they are generally not capable of reliably predicting more complex phenomena, such as shock wave–boundary layer interaction. The current status of turbulence modeling is reviewed by Wilcox (1998), Haase *et al.* (1997), Leschziner (2003), and Durbin in an article in this Encyclopedia.

Outside the boundary layer, excellent predictions can be made by treating the flow as inviscid. Setting $\sigma_{ij} = 0$ and eliminating heat conduction from equations (3, 4 and 6) yields the Euler equations for inviscid flow. These are a very useful model for predicting flows over aircraft. According to Kelvin's theorem, a smooth inviscid flow that is initially irrotational remains irrotational. This allows one to introduce a velocity potential ϕ such that $u_i = \partial\phi/\partial x_i$. The Euler equations for a steady flow now reduce to

$$\frac{\partial}{\partial x_i} \left(\rho \frac{\partial \phi}{\partial x_i} \right) = 0 \quad (37)$$

In a steady inviscid flow, it follows from the energy equation (6) and the continuity equation (3) that the total enthalpy is constant

$$H = \frac{c^2}{\gamma - 1} + \frac{1}{2} u_i u_i = H_\infty \quad (38)$$

where the subscript ∞ is used to denote the value in the far field. According to Crocco's theorem, vorticity in a steady flow is associated with entropy production through the relation

$$\mathbf{u} \times \boldsymbol{\omega} + T \nabla S = \nabla H = 0$$

where \mathbf{u} and $\boldsymbol{\omega}$ are the velocity and vorticity vectors, T is the temperature, and S is the entropy. Thus, the introduction of a velocity potential is consistent with the assumption of isentropic flow.

Substituting the isentropic relationship $p/\rho^\gamma = \text{constant}$, and the formula for the speed of sound, equation (38) can be solved for the density as

$$\frac{\rho}{\rho_\infty} = \left[1 + \frac{\gamma - 1}{2} M_\infty^2 \left(1 - \frac{u_i u_i}{u_\infty^2} \right) \right]^{1/(\gamma - 1)} \quad (39)$$

It can be seen from this equation that

$$\frac{\partial \rho}{\partial u_i} = -\frac{\rho u_i}{c^2} \quad (40)$$

and correspondingly in isentropic flow

$$\frac{\partial p}{\partial u_i} = \frac{dp}{d\rho} \frac{\partial \rho}{\partial u_i} = -\rho u_i \quad (41)$$

Substituting $(\partial \rho / \partial x_j) = (\partial \rho / \partial u_i)(\partial u_i / \partial x_j)$, the potential flow equation (37) can be expanded in quasilinear form as

$$c^2 \frac{\partial^2 \phi}{\partial x_i^2} - u_i u_j \frac{\partial^2 \phi}{\partial x_i \partial x_j} = 0 \quad (42)$$

If the flow is locally aligned, say, with the x_1 axis, equation (42) reads as

$$(1 - M^2) \frac{\partial^2 \phi}{\partial x_1^2} + \frac{\partial^2 \phi}{\partial x_2^2} + \frac{\partial^2 \phi}{\partial x_3^2} = 0 \quad (43)$$

where M is the Mach number u_1/c . The change from an elliptic to a hyperbolic partial differential equation as the flow becomes supersonic is evident.

The potential flow equation (42) also corresponds to the Bateman variational principle that the integral over the

domain of the pressure

$$I = \int_D p \, d\xi \quad (44)$$

is stationary. Here $d\xi$ denotes the volume element. Using the relation (41), a variation δp results in a variation

$$\delta I = \int_D \frac{\partial p}{\partial u_i} \delta u_i \, d\xi = - \int_D \rho u_i \frac{\partial}{\partial x_i} \delta \phi \, d\xi$$

or, on integrating by parts with appropriate boundary conditions

$$\delta I = \int_D \frac{\partial}{\partial x_i} \left(\rho \frac{\partial \phi}{\partial x_i} \right) \delta \phi \, d\xi$$

Then $\delta I = 0$ for an arbitrary variation $\delta \phi$ if equation (37) holds.

The equations of inviscid supersonic flow admit discontinuous solutions, both shock waves and contact discontinuities, which satisfy the Rankine Hugoniot jump conditions (Liepmann and Roshko, 1957). Only compression shock waves are admissible, corresponding to the production of entropy. Expansion shock waves cannot occur because they would correspond to a decrease in entropy.

Because shock waves generate entropy, they cannot be exactly modeled by the potential flow equations. The amount of entropy generated is proportional to $(M - 1)^3$ where M is the Mach number upstream of the shock. Accordingly, weak solutions admitting isentropic jumps that conserve mass but not momentum are a good approximation to shock waves, as long as the shock waves are quite weak (with a Mach number < 1.3 for the normal velocity component upstream of the shock wave). Stronger shock waves tend to separate the flow, with the result that the inviscid approximation is no longer adequate. Thus this model is well balanced, and it has proved extremely useful for the prediction of the cruising performance of transport aircraft. An estimate of the pressure drag arising from shock waves is obtained because of the momentum deficit through an isentropic jump.

If one assumes small disturbances about a free stream in the x_i direction, and a Mach number close to unity, equation (43) can be reduced to the transonic small disturbance equation in which M^2 is estimated as

$$M_\infty^2 \left[1 - (\gamma + 1) \frac{\partial \phi}{\partial x_1} \right]$$

This is the simplest nonlinear model of compressible flow.

The final level of approximation is to linearize equation (43) by replacing M^2 by its free-stream value M_∞^2 . In the subsonic case, the resulting Prandtl–Glauert equation

can be reduced to Laplace's equation by scaling the x_i coordinate by $(1 - M_\infty^2)^{1/2}$. Irrotational incompressible flow satisfies the Laplace's equation, as can be seen by setting $\rho = \text{constant}$, in equation (37). The relationships between some of the widely used mathematical models is illustrated in Figure 4. With limits on the available computing power, and the cost of the calculations, one has to make a trade-off between the complexity of the mathematical model and the complexity of the geometric configuration to be treated.

The computational requirements for aerodynamic simulation are a function of the number of operations required per mesh point, the number of cycles or time steps needed to reach a solution, and the number of mesh points needed to resolve the important features of the flow. Algorithms for the three-dimensional transonic potential flow equation require about 500 floating-point operations per mesh point per cycle. The number of operations required for an Euler simulation is in the range of 1000 to 5000 per time step, depending on the complexity of the algorithm. The number of mesh intervals required to provide an accurate representation of a two-dimensional inviscid transonic flow is of the order of 160 wrapping around the profile, and 32 normal to the airfoil. Correspondingly, about 200 000 mesh cells are sufficient to provide adequate resolution of three-dimensional inviscid transonic flow past a swept wing, and this number needs to be increased to provide a good simulation of a more complex configuration such as a complete aircraft. The requirements for viscous simulations by means of turbulence models are much more severe. Good resolution of a turbulent boundary layer needs about 32 intervals inside the boundary layer, with the result that a typical mesh for a two-dimensional Navier–Stokes calculation contains 512 intervals wrapping around the profile, and 64 intervals in the normal direction. A corresponding mesh for a swept wing would have, say, $512 \times 64 \times 256 \approx 8\,388\,608$ cells, leading to a calculation at the outer limits of current computing capabilities. The hierarchy of mathematical models is illustrated in Figure 5, while Figure 6 gives an indication of the boundaries of the complexity of problems which can be treated with different levels of computing power. The vertical axis indicates the geometric complexity, and the horizontal axis the equation complexity.

3 POTENTIAL FLOW METHODS

3.1 Boundary integral methods

The first major success in computational aerodynamics was the development of boundary integral methods for the solution of the subsonic linearized potential flow equation

$$(1 - M_\infty^2)\phi_{xx} + \phi_{yy} = 0 \quad (45)$$

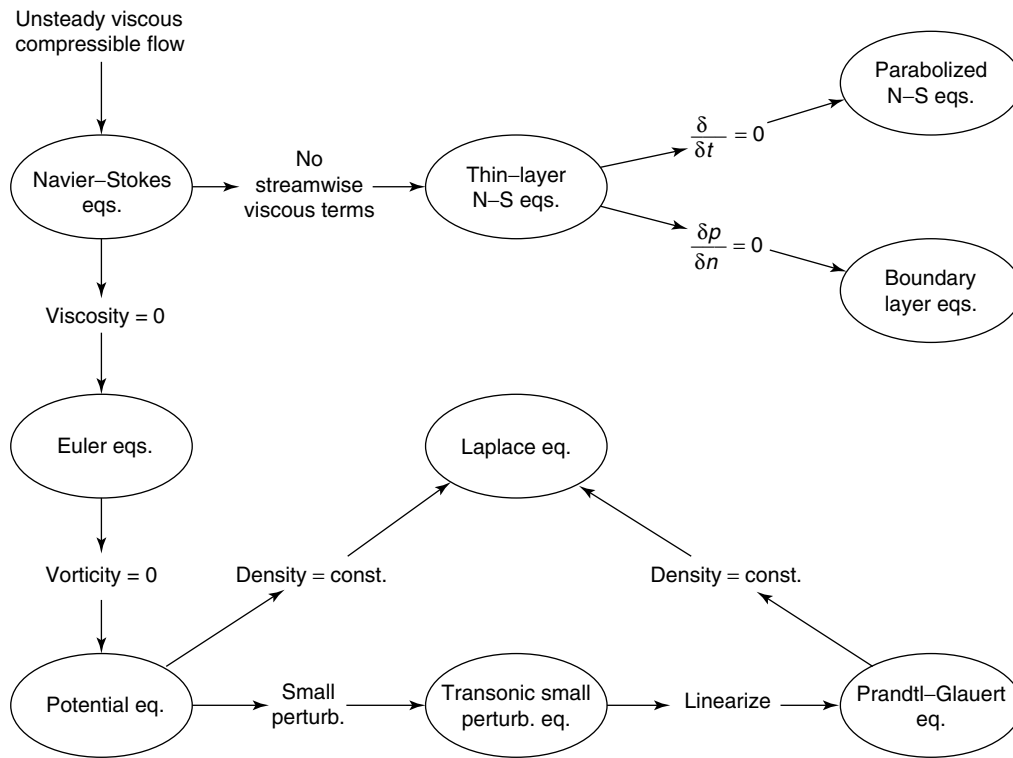


Figure 4. Equations of fluid dynamics for mathematical models of varying complexity. (Supplied by Luis Miranda, Lockheed Corporation).

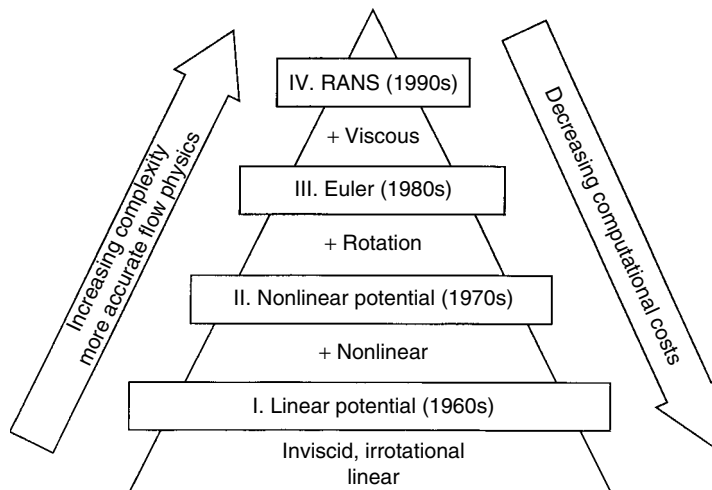


Figure 5. Hierarchy of fluid flow models.

This can be reduced to Laplace’s equation by stretching the x coordinate by the factor $\sqrt{1 - M_\infty^2}$. Then, according to potential theory, the general solution can be represented in terms of a distribution of sources or doublets, or both sources and doublets, over the boundary surface. The boundary condition is that the velocity component normal to the surface is zero. Assuming, for example, a source distribution of strength $\sigma(Q)$ at the point Q of a surface S ,

this leads to the integral equation

$$2\pi\sigma_p - \iint_S \sigma(Q)n_p \cdot \nabla \left(\frac{1}{r} \right) = 0 \quad (46)$$

where P is the point of evaluation, and r is the distance from P to Q . A similar equation can be found for a doublet distribution, and it usually pays to use a combination.

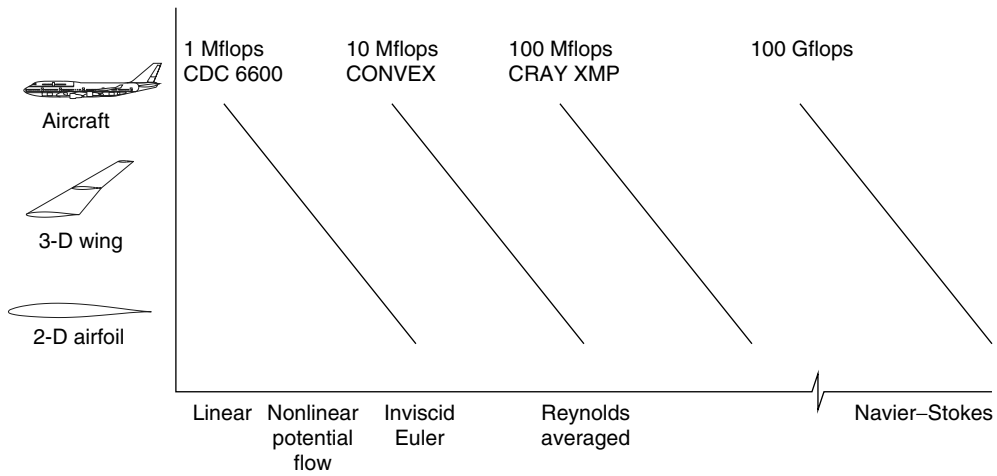


Figure 6. Complexity of the problems that can be treated with different classes of computer (1 flop = 1 floating-point operation per second; 1 Mflop = 10⁶ flops; 1 Gflop = 10⁹ flops). A color version of this image is available at <http://www.mrw.interscience.wiley.com/ecm>

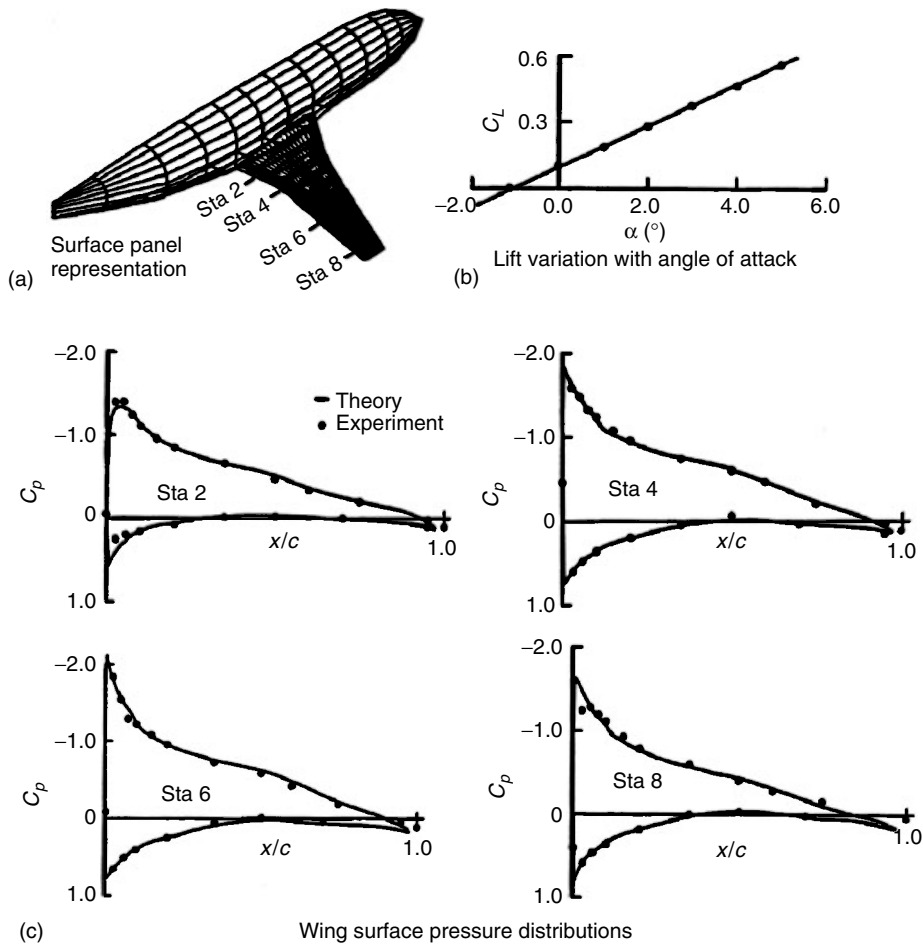


Figure 7. Panel method applied to Boeing 747. (Supplied by Paul Rubbert, the Boeing Company.)

Equation (46) can be reduced to a set of algebraic equations by dividing the surface into quadrilateral panels, assuming a constant source strength on each panel, and satisfying the condition of zero normal velocity at the center of each panel. This leads to N equations for the source strengths on N panels.

The first such method was introduced by Hess and Smith (1962). The method was extended to lifting flows, together with the inclusion of doublet distributions, by Rubbert and Saaris (1968). Subsequently higher-order panel methods (as these methods are generally called in the aircraft industry) have been introduced. A review has been given by Hunt (1978). An example of a calculation by a panel method is shown in Figure 7. The results are displayed in terms of the pressure coefficient defined as

$$c_p = \frac{p - p_\infty}{\frac{1}{2}\rho_\infty q_\infty^2}$$

Figure 8 illustrates the kind of geometric configuration that can be treated by panel methods.

In comparison with field methods, which solve for the unknowns in the entire domain, panel methods have the advantage that the dimensionality is reduced. Consider a three-dimensional flow field on an $n \times n \times n$ grid. This would be reduced to the solution of the source or doublet strengths on $N = O(n^2)$ panels. Since, however, every panel influences every other panel, the resulting equations have a dense matrix. The complexity of calculating the $N \times N$ influence coefficients is then $O(n^4)$. Also, $O(N^3) = O(n^6)$ operations are required for an exact solution. If one directly discretizes the equations for the three-dimensional domain, the number of unknowns is n^3 , but the equations are sparse and can be solved with $O(n)$ iterations or even

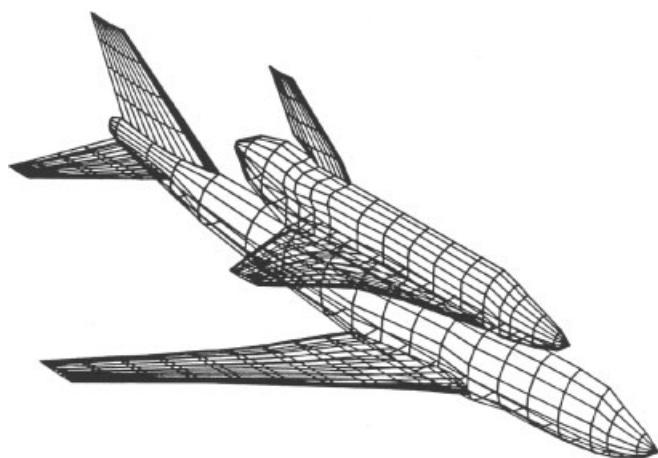


Figure 8. Panel method applied to flow around Boeing 747 and space shuttle. (Supplied by Allen Chen, the Boeing Company.)

with a number of iterations independent of n if a multigrid method is used.

Although the field methods appear to be potentially more efficient, the boundary integral method has the advantage that it is comparatively easy to divide a complex surface into panels, whereas the problem of dividing a three-dimensional domain into hexahedral or tetrahedral cells remains a source of extreme difficulty. Moreover the operation count for the solution can be reduced by iterative methods, while the complexity of calculating the influence coefficients can be reduced by agglomeration (Vassberg, 1997). Panel methods thus continue to be widely used both for the solution of flows at low Mach numbers for which compressibility effects are unimportant, and also to calculate supersonic flows at high Mach numbers, for which the linearized equation (45) is again a good approximation.

3.2 Formulation of the numerical method for transonic potential flow

The case of two-dimensional flow serves to illustrate the formulation of a numerical method for solving the transonic potential flow equation. With velocity components u, v and coordinates x, y equation (37) takes the form

$$\frac{\partial}{\partial x}(\rho u) + \frac{\partial}{\partial y}(\rho v) = 0 \quad (47)$$

The desired solution should have the property that ϕ is continuous, and the velocity components are piecewise continuous, satisfying equation (47) at points where the flow is smooth, together with the jump condition,

$$[\rho v] - \frac{dy}{dx}[\rho v] = 0 \quad (48)$$

across a shock wave, where $[]$ denotes the jump, and (dy/dx) is the slope of the discontinuity. That is to say, ϕ should be a weak solution of the conservation law (47), satisfying the condition,

$$\iint (\rho u \psi_x + \rho v \psi_y) dx dy = 0 \quad (49)$$

for any smooth test function ψ , which vanishes in the far field.

The general method to be described stems from the idea introduced by Murman and Cole (1971), and subsequently improved by Murman (1974), of using type-dependent differencing, with central-difference formulas in the subsonic zone, where the governing equation is elliptic, and upwind difference formulas in the supersonic zone,

where it is hyperbolic. The resulting directional bias in the numerical scheme corresponds to the upwind region of dependence of the flow in the supersonic zone. If we consider the transonic flow past a profile with fore-and-aft symmetry such as an ellipse, the desired solution of the potential flow equation is not symmetric. Instead it exhibits a smooth acceleration over the front half of the profile, followed by a discontinuous compression through a shock wave. However, the solution of the potential flow equation (42) is invariant under a reversal of the velocity vector, $u_i = -\phi_{x_i}$. Corresponding to the solution with a compression shock, there is a reverse flow solution with an expansion shock, as illustrated in Figure 9. In the absence of a directional bias in the numerical scheme, the fore-and-aft symmetry would be preserved in any solution that could be obtained, resulting in the appearance of improper discontinuities.

Since the quasilinear form does not distinguish between conservation of mass and momentum, difference approximations to it will not necessarily yield solutions that satisfy the jump condition unless shock waves are detected and special difference formulas are used in their vicinity. If we treat the conservation law (47), on the other hand, and preserve the conservation form in the difference approximation, we can ensure that the proper jump condition is satisfied. Similarly, we can obtain proper solutions of the small-disturbance equation by treating it in the conservation form.

The general method of constructing a difference approximation to a conservation law of the form

$$f_x + g_y = 0$$

is to preserve the flux balance in each cell, as illustrated in Figure 10. This leads to a scheme of the form

$$\frac{F_{i+1/2,j} - F_{i-1/2,j}}{\Delta x} + \frac{G_{i,j+1/2} - G_{i,j-1/2}}{\Delta y} = 0 \quad (50)$$

where F and G should converge to f and g in the limit as the mesh width tends to zero. Suppose, for example, that

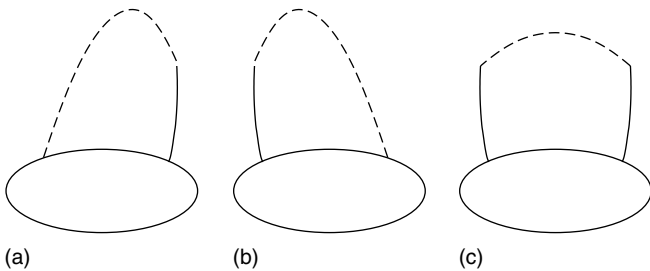


Figure 9. Alternative solutions for an ellipse. (a) Compression shock, (b) expansion shock, (c) symmetric shock.

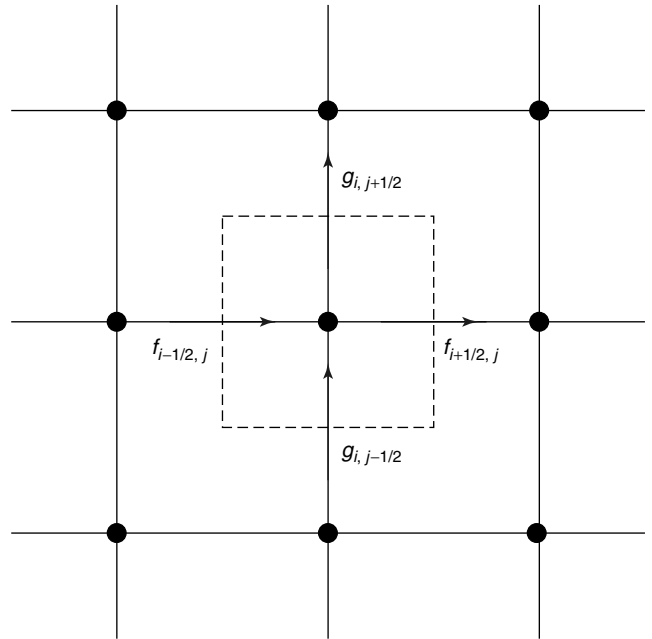


Figure 10. Flux balance of difference scheme in conservation form. A color version of this image is available at <http://www.mrw.interscience.wiley.com/ecm>

equation (50) represents the conservation law (47). Then on multiplying by a test function ψ_{ij} and summing by parts, there results an approximation to the integral (49). Thus, the condition for a proper weak solution is satisfied. Some latitude is allowed in the definitions of F and G , since it is only necessary that $F = f + O(\Delta x)$ and $G = g + O(\Delta x)$. In constructing a difference approximation, we can therefore introduce an artificial viscosity of the form

$$\frac{\partial P}{\partial x} + \frac{\partial Q}{\partial y}$$

provided that P and Q are of order Δx . Then, the difference scheme is an approximation to the modified conservation law

$$\frac{\partial}{\partial x}(f + P) + \frac{\partial}{\partial y}(g + Q) = 0$$

which reduces to the original conservation law in the limit as the mesh width tends to zero.

This formulation provides a guideline for constructing type-dependent difference schemes in conservation form. The dominant term in the discretization error introduced by the upwind differencing can be regarded as an artificial viscosity. We can, however, turn this idea around. Instead of using a switch in the difference scheme to introduce an artificial viscosity, we can explicitly add an artificial viscosity, which produces an upwind bias in the difference

scheme at supersonic points. Suppose that we have a central-difference approximation to the differential equation in conservation form. Then the conservation form will be preserved as long as the added viscosity is also in conservation form. The effect of the viscosity is simply to alter the conserved quantities by terms proportional to the mesh width Δx , which vanish in the limit as the mesh width approaches zero, with the result that the proper jump conditions must be satisfied. By including a switching function in the viscosity to make it vanish in the subsonic zone, we can continue to obtain the sharp representation of shock waves that results from switching the difference scheme.

There remains the problem of finding a convergent iterative scheme for solving the nonlinear difference equations that result from the discretization. Suppose that in the $(n + 1)$ st cycle the residual R_{ij} at the point $i\Delta x, j\Delta y$ is evaluated by inserting the result $\phi_{ij}^{(n)}$ of the n th cycle in the difference approximation. Then, the correction $C_{ij} = \phi_{ij}^{(n+1)} - \phi_{ij}^{(n)}$ is to be calculated by solving an equation of the form

$$NC + \sigma R = 0 \quad (51)$$

where N is a discrete linear operator and σ is a scaling function. In a relaxation method, N is restricted to a lower triangular or block triangular form so that the elements of C can be determined sequentially. In the analysis of such a scheme, it is helpful to introduce a time-dependent analogy. The residual R is an approximation to $L\phi$, where L is the operator appearing in the differential equation. If we consider C as representing $\Delta t\phi_t$, where t is an artificial time coordinate, and $N\Delta t$ is an approximation to a differential operator D , then equation (51) is an approximation to

$$D\phi_t + \sigma L\phi = 0 \quad (52)$$

Thus, we should choose N so that this is a convergent time-dependent process.

With this approach, the formulation of a relaxation method for solving a transonic flow is reduced to three main steps.

- Construct a central-difference approximation to the differential equation.
- Add a numerical viscosity to produce the desired directional bias in the hyperbolic region.
- Add time-dependent terms to embed the steady state equation in a convergent time-dependent process.

Methods constructed along these lines have proved extremely reliable. Their main shortcoming is a rather slow

rate of convergence. In order to speed up the convergence, we can extend the class of permissible operators N .

3.3 Solution of the transonic small-disturbance equation

3.3.1 Murman difference scheme

The basic ideas can conveniently be illustrated by considering the solution of the transonic small-disturbance equation (Ashley and Landahl, 1965)

$$[1 - M_\infty^2 - (\gamma + 1)M_\infty^2\phi_x]\phi_{xx} + \phi_{yy} = 0 \quad (53)$$

The treatment of the small-disturbance equation is simplified by the fact that the characteristics are locally symmetric about the x direction. Thus, the desired directional bias can be introduced simply by switching to upwind differencing in the x direction at all supersonic points. To preserve the conservation form, some care must be exercised in the method of switching as illustrated in Figure 11. Let p_{ij} be

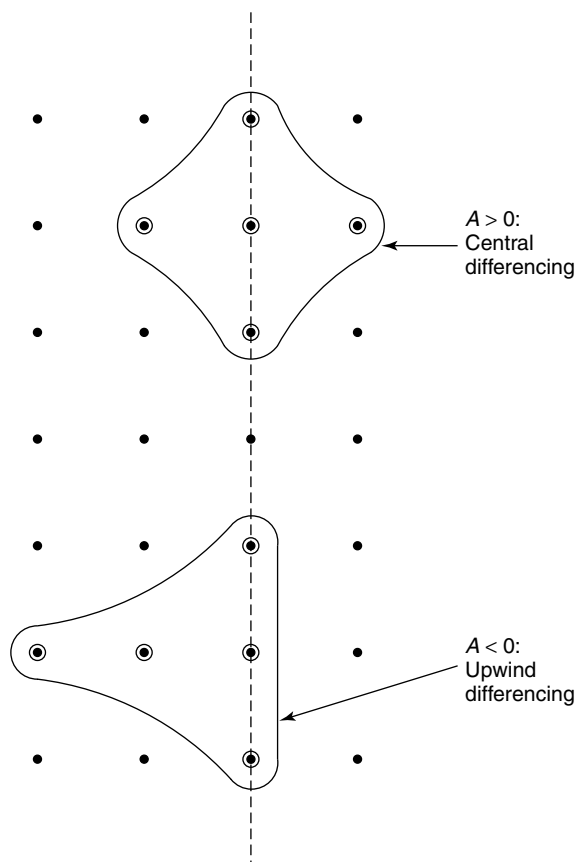


Figure 11. Murman–Cole difference scheme: $A\phi_{xx} + \phi_{yy} = 0$. A color version of this image is available at <http://www.mrw.interscience.wiley.com/ecm>

a central-difference approximation to the x derivatives at the point $i\Delta x, j\Delta y$:

$$\begin{aligned} p_{ij} &= (1 - M_\infty^2) \frac{\phi_{i+1,j} - \phi_{ij} - (\phi_{ij} - \phi_{i-1,j})}{\Delta x^2} \\ &\quad - (\gamma + 1) M_\infty^2 \frac{(\phi_{i+1,j} - \phi_{ij})^2 - (\phi_{ij} - \phi_{i-1,j})^2}{2\Delta x^3} \\ &= A_{ij} \frac{\phi_{i+1,j} - 2\phi_{ij} + \phi_{i-1,j}}{\Delta x^2} \end{aligned} \quad (54)$$

where

$$A_{ij} = (1 - M_\infty^2) - (\gamma + 1) M_\infty^2 \frac{\phi_{i+1,j} - \phi_{i-1,j}}{2\Delta x} \quad (55)$$

Also, let q_{ij} be a central-difference approximation to ϕ_{yy} :

$$q_{ij} = \frac{\phi_{i,j+1} - 2\phi_{ij} + \phi_{i,j-1}}{\Delta y^2} \quad (56)$$

Define a switching function μ with the value unity at supersonic points and zero at subsonic points:

$$\mu_{ij} = 0 \quad \text{if } A_{ij} > 0; \quad \mu_{ij} = 1 \quad \text{if } A_{ij} < 0 \quad (57)$$

Then, the original scheme of Murman and Cole (1971) can be written as

$$p_{ij} + q_{ij} - \mu_{ij}(p_{ij} - p_{i-1,j}) = 0 \quad (58)$$

Let

$$\begin{aligned} P &= \Delta x \frac{\partial}{\partial x} \left[(1 - M_\infty^2) \phi_x - \frac{\gamma + 1}{2} M_\infty^2 \phi_x^2 \right] \\ &= \Delta x A \phi_{xx} \end{aligned}$$

where A is the nonlinear coefficient defined by equation (55). Then, the added terms are an approximation to

$$-\mu \frac{\partial P}{\partial x} = -\mu \Delta x A \phi_{xxx} \quad (59)$$

This may be regarded as an artificial viscosity of order Δx , which is added at all points of the supersonic zone. Since the coefficient $-A$ of $\phi_{xxx} = u_{xx}$ is positive in the supersonic zone, it can be seen that the artificial viscosity includes a term similar to the viscous terms in the Navier–Stokes equation.

Since μ is not constant, the artificial viscosity is not in conservation form, with the result that the difference scheme does not satisfy the conditions stated in the previous section for the discrete approximation to converge to a weak solution satisfying the proper jump conditions. To correct

this, all that is required is to recast the artificial viscosity in a divergence form as $(\partial/\partial x)(\mu P)$. This leads to Murman's fully conservative scheme (Murman, 1974)

$$p_{ij} + q_{ij} - \mu_{ij} p_{ij} + \mu_{i-1,j} p_{i-1,j} = 0 \quad (60)$$

At points where the flow enters and leaves the supersonic zone, μ_{ij} and $\mu_{i-1,j}$ have different values, leading to special parabolic and shock-point equations

$$q_{ij} = 0$$

and

$$p_{ij} + p_{i-1,j} + q_{ij} = 0$$

With the introduction of these special operators, it can be verified by directly summing the difference equations at all points of the flow field that the correct jump conditions are satisfied across an oblique shock wave.

3.3.2 Solution of the difference equations by relaxation

The nonlinear difference equations (54–57, and 58 or 60) may be solved by a generalization of the line relaxation method for elliptic equations. At each point we calculate the coefficient A_{ij} and the residual R_{ij} by substituting the result ϕ_{ij} of the previous cycle in the difference equations. Then we set $\phi_{ij}^{(n+1)} = \phi_{ij}^{(n)} + C_{ij}$, where the correction C_{ij} is determined by solving the linear equations

$$\begin{aligned} &\frac{C_{i,j+1} - 2C_{i,j} + C_{i,j-1}}{\Delta y^2} \\ &+ (1 - \mu_{i,j}) A_{i,j} \frac{-(2/\omega)C_{i,j} + C_{i-1,j}}{\Delta x^2} \\ &+ \mu_{i-1,j} A_{i-1,j} \frac{C_{i,j} - 2C_{i-1,j} + C_{i-2,j}}{\Delta x^2} + R_{i,j} = 0 \end{aligned} \quad (61)$$

on each successive vertical line. In these equations, ω is the overrelaxation factor for subsonic points, with a value in the range 1 to 2. In a typical line relaxation scheme for an elliptic equation, provisional values $\tilde{\phi}_{ij}$ are determined on the line $x = i\Delta x$ by solving the difference equations with the latest available values $\phi_{i-1,j}^{(n+1)}$ and $\phi_{i+1,j}^{(n)}$ inserted at points on the adjacent lines. Then, new values $\phi_{i,j}^{(n+1)}$ are determined by the formula

$$\phi_{ij}^{(n+1)} = \phi_{ij}^{(n)} + \omega(\tilde{\phi}_{ij} - \phi_{ij}^{(n)})$$

By eliminating $\tilde{\phi}_{ij}$, we can write the difference equations in terms of $\phi_{ij}^{(n+1)}$ and $\phi_{ij}^{(n)}$. Then, it can be seen that ϕ_{yy} would

be represented by $(1/\omega)\delta_y^2\phi^{(n+1)} + [1 - (1/\omega)]\delta_y^2\phi^{(n)}$ in such a process, where δ_y^2 denotes the second central-difference operator. The appropriate procedure for treating the upwind difference formulas in the supersonic zone, however, is to march in the flow direction, so that the values $\phi_{ij}^{(n+1)}$ on each new column can be calculated from the values $\phi_{i-2,j}^{(n+1)}$ and $\phi_{i-1,j}^{(n+1)}$ already determined on the previous columns. This implies that ϕ_{yy} should be represented by $\delta_y^2\phi^{(n+1)}$ in the supersonic zone, leading to a discontinuity at the sonic line. The correction formula (61) is derived by modifying this process to remove this discontinuity. New values $\phi_{ij}^{(n+1)}$ are used instead of provisional values $\tilde{\phi}_{ij}$ to evaluate ϕ_{yy} , at both supersonic and subsonic points. At supersonic points, ϕ_{xx} is also evaluated using new values. At subsonic points, ϕ_{xx} is evaluated from $\phi_{i-1,j}^{(n+1)}$, $\phi_{i+1,j}^{(n)}$ and a linear combination of $\phi_{ij}^{(n+1)}$ and $\phi_{ij}^{(n)}$. In the subsonic zone, the scheme acts like a line relaxation scheme, with a comparable rate of convergence. In the supersonic zone, it is equivalent to a marching scheme, once the coefficients A_{ij} have been evaluated. Since the supersonic difference scheme is implicit, no limit is imposed on the step length Δx as A_{ij} approaches zero near the sonic line.

3.3.3 Nonunique solutions of the difference equations for one-dimensional flow

Some of the properties of the Murman difference formulas are clarified by considering a uniform flow in a parallel channel. Then $\phi_{yy} = 0$, and with a suitable normalization of the potential, the equation reduces to

$$\frac{\partial}{\partial x} \left(\frac{\phi_x^2}{2} \right) = 0 \tag{62}$$

with ϕ and ϕ_x given at $x = 0$, and ϕ given at $x = L$. The supersonic zone corresponds to $\phi_x > 0$. Since ϕ_x^2 is constant, ϕ_x simply reverses sign at a jump. Provided we enforce the entropy condition that ϕ_x decreases through a jump, there is a unique solution with a single jump whenever $\phi_x(0) > 0$ and $\phi(0) + L\phi_x(0) \geq \phi(L) \geq \phi(0) - L\phi_x(0)$.

Let $u_{i+1/2} = (\phi_{i+1} - \phi_i)/\Delta x$ and $u_i = (u_{i+1/2} + u_{i-1/2})/2$. Then, the fully conservative difference equations can be written as

Elliptic:

$$u_{i+1/2}^2 = u_{i-1/2}^2 \quad \text{when } u_i \leq 0 \quad u_{i-1} \leq 0 \tag{a}$$

Hyperbolic:

$$u_{i-1/2}^2 = u_{i-3/2}^2 \quad \text{when } u_i > 0 \quad u_{i-1} > 0 \tag{b}$$

Shock Point:

$$u_{i+1/2}^2 = u_{i-3/2}^2 \quad \text{when } u_i \leq 0 \quad u_{i-1} > 0 \tag{c}$$

Parabolic:

$$0 = 0 \quad \text{when } u_i > 0 \quad u_{i-1} < 0 \tag{d}$$

These admit the correct solution, illustrated in Figure 12(a) with a constant slope on the two sides of the shock. The shock-point operator allows a single link with an intermediate slope, corresponding to the shock lying in the middle of a mesh cell.

The nonconservative difference scheme omits the shock-point operator, with the result that it admits solutions of the type illustrated in Figure 12(b), with the shock too far forward and the downstream velocity too close to the sonic speed (zero with the present normalization). The direct switch in the difference scheme from (b) to (a) allows a break in the slope as long as the downstream slope is negative. The magnitude of the downstream slope cannot exceed the magnitude of the upstream slope, however, because then $u_{i-1} < 0$, and accordingly the elliptic operator would be used at the point $(i - 1)\Delta x$. Thus, the nonconservative

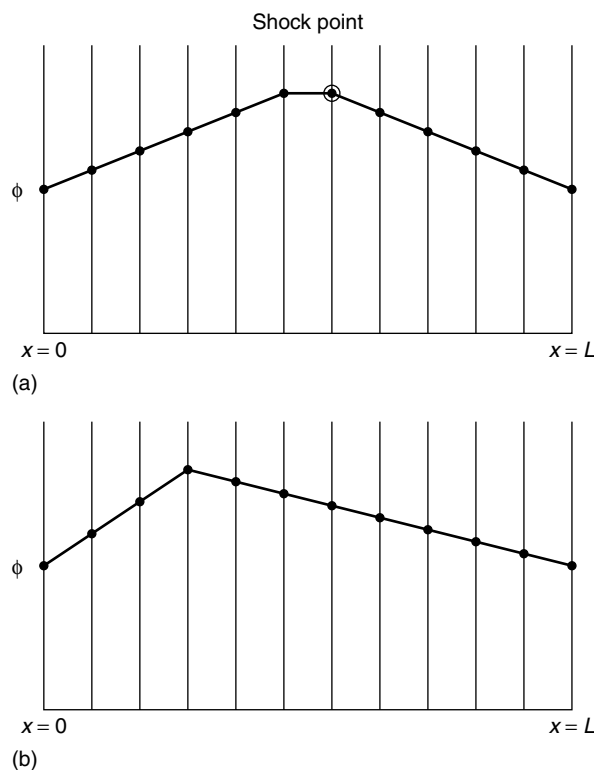


Figure 12. One-dimensional flow in a channel. • – value of ϕ at node i . A color version of this image is available at <http://www.mrw.interscience.wiley.com/ecm>

scheme enforces the weakened shock condition,

$$\phi_i - \phi_{i-2} > \phi_i - \phi_{i+2} > 0$$

which allows solutions ranging from the point at which the downstream velocity is barely subsonic up to the point at which the shock strength is correct. When the downstream velocity is too close to sonic speed, there is an increase in the mass flow. Thus, the nonconservative scheme may introduce a source at the shock wave.

The fully conservative difference equations also admit, however, various improper solutions. Figure 13(a) illustrates a sawtooth solution with u^2 constant everywhere except in one cell ahead of a shock point. Figure 13(b) illustrates another improper solution in which the shock is too far forward. At the last interior point, there is then an expansion shock that is admitted by the parabolic operator. Since the difference equations have more than one root, we must depend on the iterative scheme to find the desired root. The scheme should ideally be designed so that the correct solution is stable under a small perturbation and improper solutions are unstable. Using a scheme similar to equation (61), the instability of the sawtooth solution has been confirmed in numerical experiments. The solutions with an

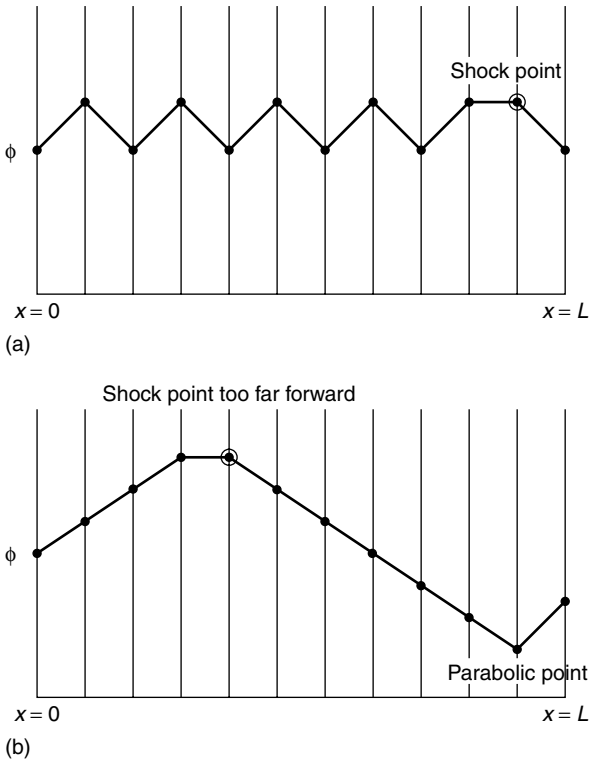


Figure 13. One-dimensional flow in a channel (a) sawtooth solution and (b) solution with downstream parabolic point. A color version of this image is available at <http://www.mrw.interscience.wiley.com/ecm>

expansion shock at the downstream boundary are stable, on the other hand, if the compression shock is too far forward by more than the width of a mesh cell. Thus there is a continuous range of stable improper solutions, while the correct solution is an isolated stable equilibrium point.

3.4 Solution of the exact potential flow equation

3.4.1 Difference schemes for the exact potential flow equation in quasilinear form

It is less easy to construct difference approximations to the potential flow equation with a correct directional bias, because the upwind direction is not known in advance. Following Jameson (1974), the required rotation of the upwind differencing at any particular point can be accomplished by introducing an auxiliary Cartesian coordinate system that is locally aligned with the flow at that point. If s and n denote the local stream-wise and normal directions, then the transonic potential flow equation becomes

$$(c^2 - q^2)\phi_{ss} + c^2\phi_{nn} = 0 \tag{63}$$

Since u/q and v/q are the local direction cosines, ϕ_{ss} and ϕ_{nn} can be expressed in the original coordinate system as

$$\phi_{ss} = \frac{1}{q^2}(u^2\phi_{xx} + 2uv\phi_{xy} + v^2\phi_{yy}) \tag{64}$$

and

$$\phi_{nn} = \frac{1}{q^2}(v^2\phi_{xx} - 2uv\phi_{xy} + u^2\phi_{yy}) \tag{65}$$

Then, at subsonic points, central-difference formulas are used for both ϕ_{ss} and ϕ_{nn} . At supersonic points, central-difference formulas are used for ϕ_{nn} , but upwind difference formulas are used for the second derivatives contributing to ϕ_{ss} , as illustrated in Figure 14.

At a supersonic point at which $u > 0$ and $v > 0$, for example, ϕ_{ss} is constructed from the formulas

$$\begin{aligned} \phi_{xx} &= \frac{\phi_{ij} - 2\phi_{i-1,j} + \phi_{i-2,j}}{\Delta x^2} \\ \phi_{xy} &= \frac{\phi_{ij} - \phi_{i-1,j} - \phi_{i,j-1} + \phi_{i-1,j-1}}{\Delta x \Delta y} \\ \phi_{yy} &= \frac{\phi_{ij} - 2\phi_{i,j-1} + \phi_{i,j-2}}{\Delta y^2} \end{aligned} \tag{66}$$

It can be seen that the rotated scheme reduces to a form similar to the scheme of Murman and Cole for the small-disturbance equation if either $u = 0$ or $v = 0$. The upwind difference formulas can be regarded as approximations

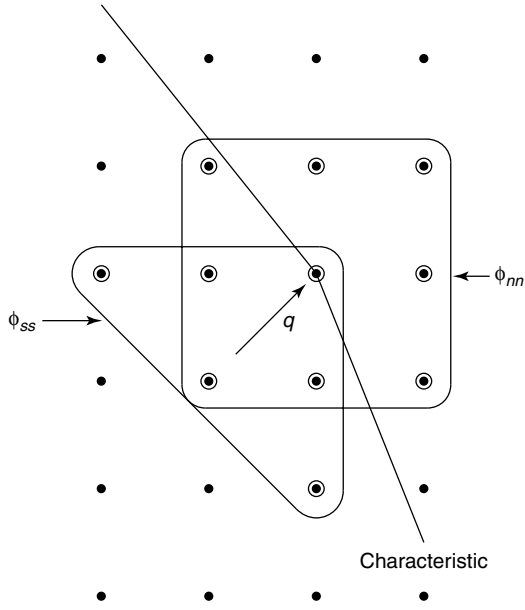


Figure 14. Rotated difference scheme.

to $\phi_{xx} - \Delta x \phi_{xxx}$, $\phi_{xy} - (\Delta x/2)\phi_{xxy} - (\Delta y/2)\phi_{xyy}$, and $\phi_{yy} - \Delta y \phi_{yyy}$. Thus at supersonic points, the scheme introduces an effective artificial viscosity

$$\left(1 - \frac{c^2}{q^2}\right) [\Delta x (u^2 u_{xx} + uv v_{xx}) + \Delta y (uv u_{yy} + v^2 v_{yy})] \quad (67)$$

which is symmetric in x and y .

3.4.2 Difference schemes for the exact potential flow equation in conservation form

In the construction of a discrete approximation to the conservation form of the potential flow equation, it is convenient to accomplish the switch to upwind differencing by the explicit addition of an artificial viscosity. Thus, we solve an equation of the form

$$S_{ij} + T_{ij} = 0 \quad (68)$$

where T_{ij} is the artificial viscosity, which is constructed as an approximation to an expression in divergence form $\partial P/\partial x + \partial Q/\partial y$, where P and Q are appropriate quantities with a magnitude proportional to the mesh width. The central-difference approximation is constructed in the natural manner as

$$S_{ij} = \frac{(\rho u)_{i+\frac{1}{2},j} - (\rho u)_{i-\frac{1}{2},j}}{\Delta x} + \frac{(\rho v)_{i,j+\frac{1}{2}} - (\rho v)_{i,j-\frac{1}{2}}}{\Delta y} \quad (69)$$

Consider first the case in which the flow in the supersonic zone is aligned with the x coordinate, so that it is sufficient to restrict the upwind differencing to the x derivatives. In a smooth region of the flow, the first term of S_{ij} is an approximation to

$$\frac{\partial}{\partial x}(\rho u) = \rho \left(1 - \frac{u^2}{c^2}\right) \phi_{xx} - \frac{\rho uv}{c^2} \phi_{xy}$$

We wish to construct T_{ij} so that ϕ_{xx} is effectively represented by an upwind difference formula when $u > c$. Define the switching function

$$\mu = \min \left[0, \rho \left(1 - \frac{u^2}{c^2}\right) \right] \quad (70)$$

Then set

$$T_{ij} = \frac{P_{i+\frac{1}{2},j} - P_{i-\frac{1}{2},j}}{\Delta x} \quad (71)$$

where

$$P_{i+\frac{1}{2},j} = -\frac{\mu_{ij}}{\Delta x} [\phi_{i+1,j} - 2\phi_{ij} + \phi_{i-1,j} - \epsilon(\phi_{ij} - 2\phi_{i-1,j} + \phi_{i-2,j})] \quad (72)$$

The added terms are an approximation to $\partial P/\partial x$, where

$$P = -\mu[(1 - \epsilon)\Delta x \phi_{xx} + \epsilon \Delta x^2 \phi_{xxx}]$$

Thus, if $\epsilon = 0$, the scheme is first-order accurate; but if $\epsilon = 1 - \lambda \Delta x$ and λ is a constant, the scheme is second-order accurate. Also, when $\epsilon = 0$ the viscosity cancels the term $\rho(1 - u^2/c^2)\phi_{xx}$ and replaces it by its value at the adjacent upwind point.

In this scheme, the switch to upwind differencing is introduced smoothly because the coefficient $\mu \rightarrow 0$ as $u \rightarrow c$. If the first term in S_{ij} were simply replaced by the upwind difference formula

$$\frac{(\rho u)_{i-\frac{1}{2},j} - (\rho u)_{i-\frac{3}{2},j}}{\Delta x}$$

the switch would be less smooth because there would also be a sudden change in the representation of the term $(\rho uv/c^2)\phi_{xy}$, which does not necessarily vanish when $u = c$. A scheme of this type proved to be unstable in numerical tests.

The treatment of flows that are not well aligned with the coordinate system requires the use of a difference scheme in which the upwind bias conforms to the local flow direction. The desired bias can be obtained by modeling the added terms T_{ij} on the artificial viscosity of the rotated difference

scheme for the quasilinear form described in the previous section. Since equation (47) is equivalent to equation (63) multiplied by ρ/c^2 , P and Q should be chosen so that $\partial P/\partial x + \partial Q/\partial y$ contains terms similar to equation (67) multiplied by ρ/c^2 . The following scheme has proved successful. Let μ be a switching function that vanishes in the subsonic zone:

$$\mu = \max \left[0, \left(1 - \frac{c^2}{q^2} \right) \right] \quad (73)$$

Then, P and Q are defined as approximations to

$$-\mu \left[(1 - \epsilon)u \Delta x \rho_x + \epsilon u \Delta x^2 \rho_{xx} \right]$$

and

$$-\mu \left[(1 - \epsilon)v \Delta y \rho_y + \epsilon v \Delta y^2 \rho_{yy} \right]$$

where the parameter ϵ controls the accuracy in the same way as in the simple scheme. If $\epsilon = 0$, the scheme is first-order accurate, and at a supersonic point where $u > 0$ and $v > 0$, P then approximates

$$-\Delta x \left(1 - \frac{c^2}{q^2} \right) u \rho_x = \Delta x \frac{\rho}{c^2} \left(1 - \frac{c^2}{q^2} \right) (u^2 u_x + uv v_x)$$

When this formula and the corresponding formula for Q are inserted in $\partial P/\partial x + \partial Q/\partial y$, it can be verified that the terms containing the highest derivatives of ϕ are the same as those in equation (67) multiplied by ρ/c^2 . In the construction of P and Q , the derivatives of P are represented by upwind difference formulas. Thus, the formula for the viscosity finally becomes

$$T_{ij} = \frac{P_{i+\frac{1}{2},j} - P_{i-\frac{1}{2},j}}{\Delta x} + \frac{Q_{i,j+\frac{1}{2}} - Q_{i,j-\frac{1}{2}}}{\Delta y} \quad (74)$$

where if $u_{i+1/2,j} > 0$, then

$$P_{i+\frac{1}{2},j} = u_{i+\frac{1}{2},j} \mu_{ij} \left[\rho_{i+\frac{1}{2},j} - \rho_{i-\frac{1}{2},j} - \epsilon (\rho_{i-\frac{1}{2},j} - \rho_{i-\frac{3}{2},j}) \right]$$

and if $u_{i+1/2,j} < 0$, then

$$P_{i+\frac{1}{2},j} = u_{i+\frac{1}{2},j} \mu_{i+1,j} \left[\rho_{i+\frac{1}{2},j} - \rho_{i+\frac{3}{2},j} - \epsilon (\rho_{i+\frac{3}{2},j} - \rho_{i+\frac{5}{2},j}) \right]$$

while $Q_{i,j+1/2}$ is defined by a similar formula.

3.4.3 Analysis of the relaxation method

Both the nonconservative rotated difference scheme and the difference schemes in conservation form lead to difference equations that are not amenable to solution by marching in the supersonic zone, and a rather careful analysis is needed to ensure the convergence of the iterative scheme. For this purpose, it is convenient to introduce the time-dependent analogy proposed in Section 3.2. Thus, we regard the iterative scheme as an approximation to the artificial time-dependent equation (52). It was shown by Garabedian (1956) that this method can be used to estimate the optimum relaxation factor for an elliptic problem.

To illustrate the application of the method, consider the standard difference scheme for Laplace's equation. Typically, in a point overrelaxation scheme, a provisional value $\tilde{\phi}_{ij}$ is obtained by solving

$$\frac{\phi_{i-1,j}^{(n+1)} - 2\tilde{\phi}_{ij} + \phi_{i+1,j}^{(n)}}{\Delta x^2} + \frac{\phi_{i,j-1}^{(n+1)} - 2\tilde{\phi}_{ij} + \phi_{i,j+1}^{(n)}}{\Delta y^2} = 0$$

Then the new value $\phi_{ij}^{(n+1)}$ is determined by the formula

$$\phi_{ij}^{(n+1)} = \phi_{ij}^{(n)} + \omega (\tilde{\phi}_{ij} - \phi_{ij}^{(n)})$$

where ω is the overrelaxation factor. Eliminating $\tilde{\phi}_{ij}$, this is equivalent to calculating the correction $C_{ij} = \phi_{ij}^{(n+1)} - \phi_{ij}^{(n)}$ by solving

$$\tau_1 (C_{ij} - C_{i-1,j}) + \tau_2 (C_{ij} - C_{i,j-1}) + \tau_3 C_{i,j} = R_{ij} \quad (75)$$

where R_{ij} is the residual, and

$$\tau_1 = \frac{1}{\Delta x^2}$$

$$\tau_2 = \frac{1}{\Delta y^2}$$

$$\tau_3 = \left(\frac{2}{\omega} - 1 \right) \left(\frac{1}{\Delta x^2} + \frac{1}{\Delta y^2} \right)$$

Equation (75) is an approximation to the wave equation

$$\tau_1 \Delta t \Delta x \phi_{xt} + \tau_2 \Delta t \Delta y \phi_{yt} + \tau_3 \Delta t \phi_t = \phi_{xx} + \phi_{yy}$$

This is damped if $\tau_3 > 0$, and to maximize the rate of convergence, the relaxation factor ω should be chosen to give an optimal amount of damping.

If we consider the potential flow equation (63) at a subsonic point, these considerations suggest that the scheme (75), where the residual R_{ij} is evaluated from the difference

approximation described in Section 3.4.1, will converge if

$$\tau_1 \geq \frac{c^2 - u^2}{\Delta x^2}, \quad \tau_2 \geq \frac{c^2 - v^2}{\Delta y^2}, \quad \tau_3 > 0$$

Similarly, the scheme

$$\tau_1(C_{ij} - C_{i-1,j}) + \tau_2(C_{i,j+1} - 2C_{ij} + C_{i,j-1}) + \tau_3 C_{i,j} = R_{ij} \quad (76)$$

which requires the simultaneous solution of the corrections on each vertical line, can be expected to converge if

$$\tau_1 \geq \frac{c^2 - u^2}{\Delta x^2}, \quad \tau_2 = \frac{c^2 - v^2}{\Delta y^2}, \quad \tau_3 > 0$$

At supersonic points, schemes similar to (75) or (76) are not necessarily convergent (Jameson, 1974). If we introduce a locally aligned Cartesian coordinate system and divide through by c^2 , the general form of the equivalent time-dependent equation is

$$(M^2 - 1)\phi_{ss} - \phi_{nn} + 2\alpha\phi_{st} + 2\beta\phi_{nt} + \gamma\phi_t = 0 \quad (77)$$

where M is the local Mach number, and s and n are the stream-wise and normal directions. The coefficients α , β , and γ depend on the coefficients of the elements of C on the left-hand side of (75) and (76). The substitution

$$T = t - \frac{\alpha s}{M^2 - 1} + \beta n$$

reduces this equation to the diagonal form

$$(M^2 - 1)\phi_{ss} - \phi_{nn} - \left(\frac{\alpha^2}{M^2 - 1} - \beta^2 \right) \phi_{TT} + \gamma\phi_T = 0$$

Since the coefficients of ϕ_{nn} and ϕ_{ss} have opposite signs when $M > 1$, T cannot be the time-like direction at a supersonic point. Instead, either s or n is time-like, depending on the sign of the coefficient of ϕ_{TT} . Since s is the time-like direction of the steady state problem, it ought also to be the time-like direction of the unsteady problem. Thus, when $M > 1$, the relaxation scheme should be designed so that α and β satisfy the compatibility condition

$$\alpha > \beta\sqrt{M^2 - 1} \quad (78)$$

The characteristics of the unsteady equation (77) satisfy

$$(M^2 - 1)(t^2 + 2\beta nt) - 2\alpha st - (\beta s - \alpha n)^2 = 0$$

Thus, the characteristic cone touches the s - n plane. As long as condition (78) holds with $\alpha > 0$ and $\beta > 0$, it slants upstream in the reverse time direction, as illustrated in Figure 15. To ensure that the iterative scheme has the

proper region of dependence, the flow field should be swept in a direction such that the updated region always includes the upwind line of tangency between the characteristic cone and the s - n plane.

A von Neumann analysis (Jameson, 1974) indicates that the coefficient of ϕ_t should be zero at supersonic points, reflecting the fact that t is not a time-like direction. The mechanism of convergence in the supersonic zone can be inferred from Figure 15. An equation of the form of (78) with constant coefficients reaches a steady state because with advancing time the cone of dependence ceases to intersect the initial time plane. Instead, it intersects a surface containing the Cauchy data of the steady state problem. The rate of convergence is determined by the backward inclination of the most retarded characteristic

$$t = \frac{2\alpha s}{M^2 - 1}, \quad n = -\frac{\beta}{\alpha}s$$

and is maximized by using the smallest permissible coefficient α for the term in ϕ_{st} . In the subsonic zone, on the other hand, the cone of dependence contains the t axis, and it is important to introduce damping to remove the influence of the initial data.

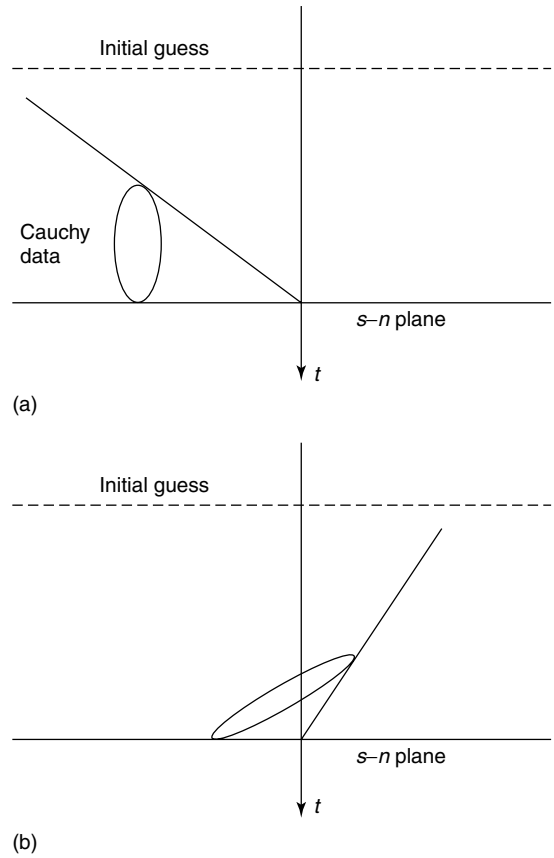


Figure 15. Characteristic cone of equivalent time-dependent equation. (a) Supersonic, (b) subsonic.

3.5 Treatment of complex geometric configurations

An effective approach to the treatment of two-dimensional flows over complex profiles is to map the exterior domain conformally onto the unit disk (Jameson, 1974). Equation (47) is then written in polar coordinates as

$$\frac{\partial}{\partial \theta} \left(\frac{\rho}{r} \phi_{\theta} \right) + \frac{\partial}{\partial r} (r \rho \phi_r) = 0 \quad (79)$$

where the modulus h of the mapping function enters only in the calculation of the density from the velocity

$$\mathbf{q} = \frac{\nabla \phi}{h} \quad (80)$$

The Kutta condition is enforced by adding circulation such that $\nabla \phi = 0$ at the trailing edge. This procedure is very accurate. Figure 16 shows a numerical verification of Morawetz's theorem that a shock-free transonic flow is an isolated point, and that arbitrary small changes in boundary conditions will lead to the appearance of shock waves (Morawetz, 1956). These calculations were performed by the author's program flo6.

Applications to complex three-dimensional configurations require a more flexible method of discretization, such as that provided by the finite element method. Jameson and Caughey proposed a scheme using isoparametric bilinear or trilinear elements (Jameson and Caughey, 1977; Jameson, 1978). The discrete equations can most conveniently

be derived from the Bateman variational principle. In the scheme of Jameson and Caughey, I is approximated as

$$I = \sum p_k V_k$$

where p_k is the pressure at the center of the k th cell and V_k is its area (or volume), and the discrete equations are obtained by setting the derivative of I with respect to the nodal values of potential to zero. Artificial viscosity is added to give an upwind bias in the supersonic zone, and an iterative scheme is derived by embedding the steady state equation in an artificial time-dependent equation. Several widely used codes (flo27, flo28, flo30) have been developed using this scheme. Figure 17 shows a result for a swept wing.

An alternative approach to the treatment of complex configurations has been developed by Bristeau *et al.* (1980a); Bristeau *et al.* (1980b). Their method uses a least squares formulation of the problem, together with an iterative scheme derived with the aid of optimal control theory. The method could be used in conjunction with a subdivision into either quadrilaterals or triangles, but in practice triangulations have been used.

The simplest conceivable least squares formulation calls for the minimization of the objective function

$$I = \int_S \psi^2 dS$$

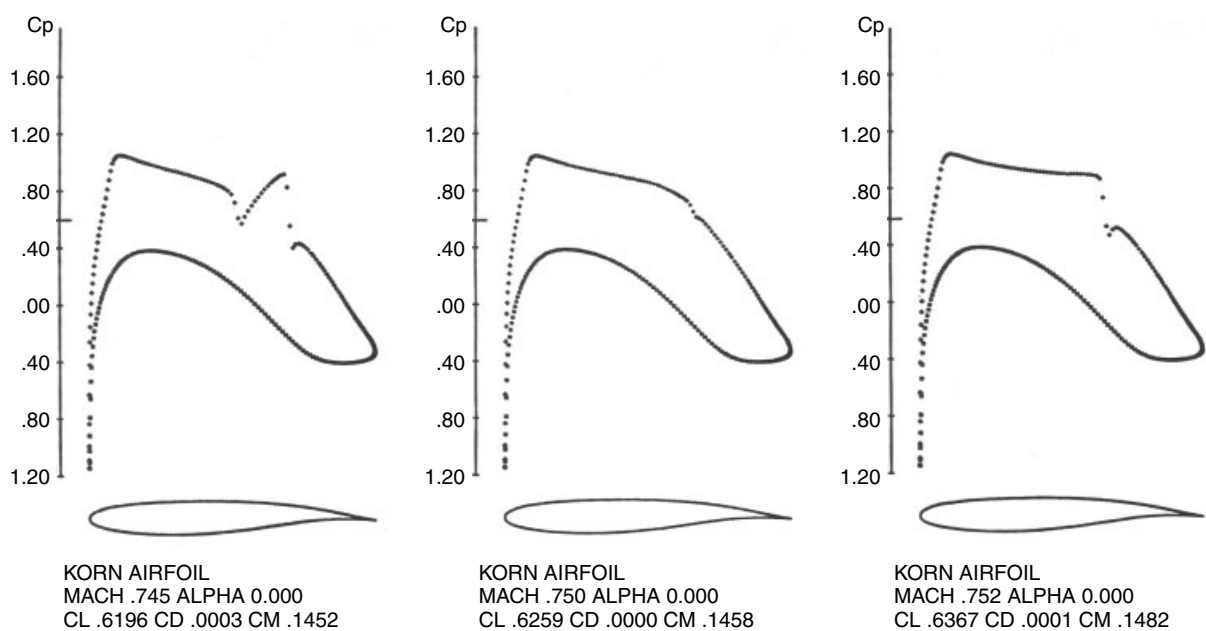


Figure 16. Sensitivity of a shock-free solution.

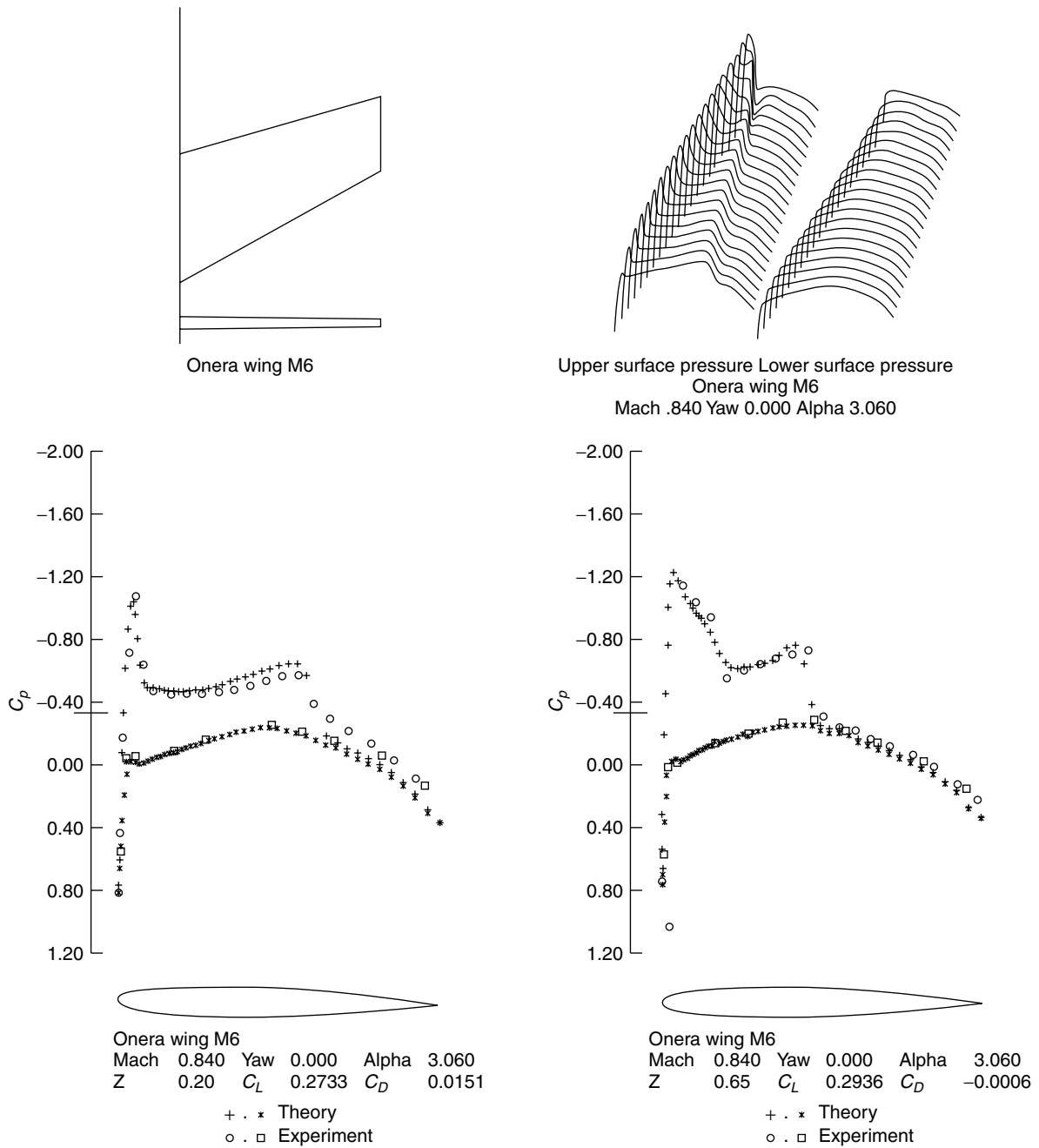


Figure 17. Swept wing.

where ψ is the residual of equation (47) and S is the domain of the calculation. The resulting minimization problem could be solved by a steepest descent method in which the potential is repeatedly modified by a correction $\delta\phi$ proportional to $(\partial I/\partial\phi)$. Such a method would be very slow. In fact, it simulates a time-dependent equation of the form

$$\phi_t = -L^*L\phi$$

where L is the differential operator in equation (47), and L^* is its adjoint. Much faster convergence can be obtained by the introduction of a more sophisticated objective function

$$I = \int_S \nabla\psi^2 dS$$

where the auxiliary function ϕ is calculated from

$$\nabla^2\psi = \nabla \cdot (\rho\nabla\phi)$$

Let g be the value of $(\partial\phi/\partial n)$ specified on the boundary C of the domain. Then, this equation can be replaced by the corresponding variational form

$$\int_S \nabla\psi \cdot \nabla v \, dS = \int_S \rho \nabla \cdot \nabla v \, dS - \int_C g v \, dS$$

which must be satisfied by ψ for all differentiable test functions v . This formulation, which is equivalent to the use of an H^{-1} norm in Sobolev space, reduces the calculation of the potential to the solution of an optimal control problem, with ϕ as the control function and ψ as the state function. It leads to an iterative scheme that calls

for solutions of Poisson equations twice in each cycle. A further improvement can be realized by the use of a conjugate gradient method instead of a simple steepest descent method.

The least squares method in its basic form allows expansion shocks. In early formulations, these were eliminated by penalty functions. Subsequently, it was found best to use upwind biasing of the density. The method has been extended at Avions Marcel Dassault to the treatment of extremely complex three-dimensional configurations, using a subdivision of the domain into tetrahedra (Bristeau *et al.*, 1985).